(FFPE) biopsies and resections were evaluated by a pathologist prior to microdissection. DNA was extracted using Qiagen QIAamp FFPE Tissue kits. IDH1/IDH2 mutation analysis was done by Sequenom mass spectrometry (MS) using lab developed PCR and extension primers, designed using Sequenom software. MS peaks were manually read from the MassARRAY Analyzer 4 system.

Results: The mean age of patients was 62 years (39–85). Males represented 31 of 57 (54%) of the overall specimens, and 16 of 39 (41%) for IHCC. In IHCC, 3 of 39 cases (7.6%) had an IDH1 394C>T mutation. In EHCC, 0 of 11 cases contained IDH mutations and 0 of 7 HCC cases. All 3 of the IDH mutated cases were female. In the three IDH1 mutated IHCCs, 1 patient had disease progression despite surgical resection and chemotherapy, 1 had disease progression with surgery alone and 1 is currently disease free following surgical resection alone.

Conclusions: In our patient population**,** the frequency of IDH mutations, 7.6% is lower than some of those reported in the literature. The mutation was limited to IDH1 394C>T and all 3 cases were female with different treatments and clinical outcomes. Identification of the IDH mutation may provide an additional therapeutic approach in cholangiocarcinoma patients who harbor this mutation.

1819 Expression of Estrogen Receptor beta Isoforms in Pancreatic Adenocarcinoma

Mamoun Younes, Charles J Ly, Kanchan Singh, Atilla Ertan, Sushovan Guha, Pamela S Younes, Jennifer M Bailey. University of Texas Health Science Center at Houston McGovern Medical School, Houston, TX.

Background: There have been several limited trials in which tamoxifen efficacy was tested in patients with pancreatic adenocarcinoma (PAC). Most of these studies were small series of patients with unresectable PAC and reported mixed results. In these studies, patients were not stratified by estrogen receptor status because estrogen receptor beta (ER-b) had not yet been identified, and PAC did not express the traditional ER-alpha. Recent studies showed that the effects of estrogens, phytoestrogens and tamoxifen on PAC cell lines depended on ER-b expression. The aim of this study was to investigate ER-b expression in human PAC and whether such expression correlates with any clinicopathologic parameters.

Design: Sections of tissue microarray containing 18 formalin fixed and paraffin embedded human PAC were stained by immunohistochemistry (IHC) using monoclonal antibodies to ER-b isoforms 1, 2, and 5 (ER-b1, ER-b2, and ER-b5, respectively), and for Cyclin A. The levels of ER-b isoform expression in tumor cells and the S-phase fraction (SPF) were determined using a quantitative digital image analysis.

Results: All ER-b isoforms were expressed in PAC, although at different levels. Higher mean ER-b2 levels correlated with male sex (p=0.057), older age (p=0.005), and lower pT stage (p=0.008), but not with grade, pN stage, or SPF. Mean ER-b5 levels correlated negatively with SPF (p=0.021), but not with sex, age, grade, pT or pN. Mean ER-b1 expression did not correlate with any of the above mentioned clinicopathologic factors.

Conclusions: ER-b1, ER-b2, and ER-b5 are expressed in PAC. Higher ER-b2 and ER-b5 levels of expression are significantly correlated with lower tumor pT stage and with lower SPF, respectively, suggesting that they may play a tumor suppressive role in PAC. The association between ER-b2 levels and patient sex and age suggest that it could be influenced by endogenous/exogenous hormonal exposure.

1820 Molecular Analysis of Pancreatic Malignant Serous Cystic Tumors by Targeted Next Generation Sequencing

Hongfa Zhu, Huai-Bin Mabel Ko, Alexandros D Polydorides, Noam Harpaz, John T Fallon, Minghao Zhong. Icahn School of Medicine at Mount Sinai, New York, NY; Westchester Medical Center, Valhalla, NY.

Background: Pancreatic serous cystadenocarcinoma (SCAC) is a rare controversial entity that is morphologically indistinguishable from benign serous cystadenoma (SCA). Recent studies suggested that half of SCAs harbor mutations in the VHL gene and contain an average of 10 somatic mutations per tumor compared to 48 somatic mutations in pancreatic adenocarcinoma. However, little is known about the molecular landscape of SCAC and its underlying tumorigenesis.

We aimed to study the genetic alterations in SCAC using targeted next generation sequence (NGS).

Design: We retrieved cases of resected SCACs and control SCA from our records. Macrodissection of formalin-fixed paraffin-embedded (FFPE) tissue corresponding to H&E-stained slides was used to ensure least 20% neoplastic cells. Genomic DNA was extracted (Qiagen AllPrep) and subjected to targeted NGS (Illumina TruSeq Amplicon) , which includes 48 cancer-associated genes.

Results: Three SCACs (2 female, 1 male, mean age 69 years) were identified. Two of them showed local gross invasion, perineural, lymph node invasion, or liver metastasis; and the third one had malignant histomorphology

Two of three SCACs had positive results including APC and ATM mutations as well as mutations in the receptor tyrosine kinase family (ERBB-4, ABL1, KIT, CSF1R), tumor suppressor genes (PTEN), and other signal transduction genes (GNAQ, KDR, HRAS). In contrast, the benign SCA control case only showed APC and VHL mutations.

	age (yr)	sex	size (cm)	inva-sion	mets	followup	mutations
SCA	81	F	3.1	no	no	n/a	APC, VHL
SCAC1	69	F	5.5	yes	node	n/a	APC, ATM, ERBB4, GNAQ, KIT, PTEN, HRAS
SCAC2	79	F	4	no	liver, node	16yr, alive	n/a
SCAC3	60	M	3	no	node	1yr	APC, ATM, ABL1, CSF1R, KDR

Molecular alterations important in pancreatic adenocarcinoma such as Kras, p16, p53, or SMAD4 were absent from SCACs.

Conclusions: SCACs are characterized by shared APC mutations with SCAs, suggesting a possible early role in tumorigenesis. In addition, SCACs lack VHL mutations (commonly seen in SCAs) but share mutations in ATM and other genes involved in signal transduction. Further studies are warranted to confirm the role of these genes in SCACs and identify potential future treatment targets.

Pathobiology (including Pan-genomic/ Pan-proteomic approaches to cancer)

1821 Detection of Somatic Mutations in Histologically Normal Lung Tissue: Sectioning and Genomic Method

Behnoush Abedi-Ardekani, Patrice H Avogbe, Matthieu Foll, Magali Olivier, Christine Carreira, Ghislaine Scelo, James D McKay. International Agency for Research on Cancer, Lyon, France.

Background: Recent studies have shown the presence of evolving clones carrying cancer-causing mutations in the benign or premalignant lesions and even histologically normal epithelium. Here, we provide proof of principle of a method for the sensitive detection of *TP53* somatic mutations within histologically normal lung tissues.

Design: Our method was as follows:

i) Appropriate sampling to obtain cells of clonal origin

Step 1: Two pieces of fresh frozen normal lung tissues of two patients with lung tumors and different smoking habits (ex-smoker and heavy smoker) were mapped microscopically to obtain fifteen 1-mm punch biopsies from each. All punches proceeded separately for DNA extraction and sequencing (n=30).

Step 2: Four more punches were taken from the ex-smoker patient, each embedded in OCT, cut to 25-30 sections of 40µm and sequenced separately (n=110). One 1mm punch biopsy of each patient's tumor was equally analyzed (n=64).

ii) Sequencing

We applied a sensitive targeted sequencing protocol specially designed for low-input DNA. 10ng DNA from each punch or section was used for targeted enrichment followed by 10,000X sequencing of *TP53* by Ion Torrent™ Proton sequencer. Each sample was sequenced as a duplicate. Only variants found in both libraries were considered for final analysis.

iii) Data analysis

We used needlestack pipeline, an ultra-sensitive caller to reliably identify variants in very low allelic fractions (AF)(https://github.com/IARCbioinfo/needlestack) and we applied a functional filter based on IARC *TP53* database (http://p53.iarc.fr/).

Results: Three different Protein-altering *TP53* mutations were detected in the ex-smoker patient, summarized below. One of them was found in the assay step 2 and in several successive sections (22-30 in punch 3 and 2-25 in punch 4) that supports a clonal expansion event. None of these mutations were detected in tumor samples.

Assay step	Punch No.	Section level	Mutation effec	Mutation type	Exon	Protein descriptiona	%AFb
1	2	N/A	Missense	G:C>A:T	8	p.C227Y	06
1	11	N/A	nonsense	G:C>A:T	6	p.Q192*	0.3
2			Missense	G:C>A:T at CpG	8	p.R273H	1-7
aReference sequence: NM_000546							
bSimilar AF between library duplicates							

Conclusions: Our findings suggest that our sectioning and genomic method is capable to detect somatic *TP53* mutations in histologically normal tissue. However, further analyses are needed with bigger sample size to confirm it.

1822 Biological Aggressiveness of Thyroid Neoplasia Depends on the Strength of the Genetic Mutation and Associated Cellular Interaction

Anna Banizs, Joseph F Annunziata, Christina M Narick, Sara Jackson, Jan F Silverman, Sydney Finkelstein. Allegheny General Hospital, Pittsburgh, PA; Interpace Diagnostics, Pittsburgh, PA.

Background: Neoplasia of the thyroid can harbor a variety of genetic mutations displaying a range of biological aggressiveness across the benign to malignant spectrum. To better understand the mechanistic basis for this differential aggressiveness we analyzed a large database of thyroid nodule aspirates (n=3341) by cytology, mutational and microRNA (miRNA) classifier analysis.

Design: Cytology diagnosis was based on cytology reports submitted using Bethesda Diagnostic Categories (BDC- I to VI). Separate needle passes were used for molecular testing. Mutational analysis encompassed common mutations (*BRAF*, *RAS*, *PIK3CA, PAX8/PPARγ* and *RET/PTC* translocations) on next generation sequencing (NGS) platform (Illumina). Variant sequence content (%) on NGS was quantified for each detectable oncogene point mutation. The miRNA classifier utilized a 10 miRNA panel trained on 257 thyroid reactive, benign, malignant. Diagnostic modalities underwent statistical comparison using ANOVA on Ranks.

Results: miRNA classifier results yielded a quantitative measure across the benign/ malignant continuum assigned to four cancer risk categories: very low (n=830) with 99+% NPV, low (n=1962) with 94% NPV, moderate (n=372) with 74% PPV and high (n=177) with 99+% PPV. NGS mutational analysis, using the miRNA classifier as the gold standard, showed clear differences between strong (*BRAFV600E*), intermediate (i.e. other *BRAF*s) and weak (*RAS*) driver mutations. Differential properties were also demonstrated within the *RAS* gene, with *NRAS* (n=279) and *HRAS* (n=125) statistically

stronger than *KRAS* (n=79, p <0.05). Mutation variant sequence percentage varied from non-detectable to 100%. Strong driver mutations tended to be clonally expanded and associated with higher risk miRNA classifier status even with low percentage of mutated copy (<5%).

Conclusions: Acquired mutations in early stages of follicular neoplastic progression are heterogeneously distributed and clonally expanded to varying degree. Classifier status is causally related to mutation type however each nodule appears to consist of a mixture of mutated and non-mutated cells exhibiting similar cellular morphology. Strong driver mutations represented in very low copy numbers appear able to recruit non-mutated cells more effectively compared to weak mutations supporting a critical role for intracellular communication likely mediated through exosomes.

1823 Adequacy of the Oncomine Comprehensive Panel for Identifying Potentially Actionable Mutations in Triple Negative Breast Carcinomas

Jordan E Baum, Pan Zhang, Sandra J Shin, Hung Tran, Xiaojun Feng, Helen Fernandes. Weill Cornell Medicine, New York, NY.

Background: The Oncomine Comprehensive Panel (OCP) is a multiplexed PCR-based next generation sequencing (NGS) assay system to identify potential treatment strategies from predefined somatic solid tumor genome variants. The OCP is advantageous over more costly and labor intensive molecular methods, such as whole exome sequencing, because the panel is compatible with Ion Torrent NGS workflow. Importantly, genes without near-term clinical actionability are excluded. While currently limited to research use only, the OCP is directly aligned with the NCI-MATCH trial. The aim of our study is to investigate the use of the OCP on archival formalin-fixed paraffin embedded (FFPE) tissue using a cohort of triple negative breast carcinomas.

Design: 30 cases of triple negative breast carcinoma excisions were identified from 2004 to 2015 in our specimen archives including 29 cases of invasive ductal carcinoma (26 poorly- and 3 moderately-differentiated) and 1 metaplastic carcinoma. Two 1 mm diameter cores were prepared from each FFPE tissue block. Extracted DNA and RNA were subjected to targeted NGS using the OCP and Ion Torrent platform, interrogating 73 cancer hotspots (single nucleotide variants (SNVs) and small insertions and deletions (INDELs)), 75 copy number variants (CNVs) and 22 fusion drivers. Data analysis was performed using the Ion Reporter v 5.0.

Results: Average DNA and RNA concentrations were 43 ng/mL and 30 ng/mL, respectively. 100% of cases were successfully sequenced. Genetic alterations were identified in 93% of cases. 17/30 cases showed CNAs, 25/30 showed SNVs and 6/30 showed INDELS. SNVs and INDELs showed an average depth of coverage of 1196X and an average allele ratio of 0.43. The most commonly encountered hotspot mutations were *TP53* (n=19) and *PIK3CA* (n=5). *MCL1* (n=8), *MYC* (n=7) and *FGFR2* (n=3) were the most common amplifications while *TET2*, *PIK3R1*, *PTEN* and *CDKN2A* were the most common deletions (n=3 each). No fusions were identified. Alterations that would enable enrollment in a NCI-MATCH treatment arm were identified in 15 cases.

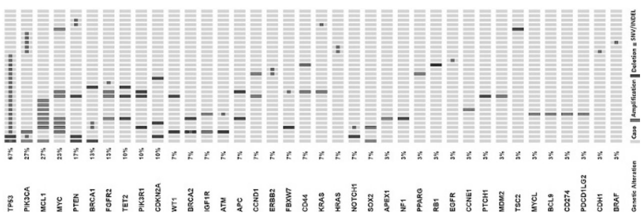

Conclusions: The OCP successfully identified genetic alterations with clinical actionability or near-term clinical actionability in FFPE specimens of triple negative breast carcinomas.

1824 Clinical Value of Larger Multi-Gene Next-Generation Sequencing Panels

Russell R Broaddus, Beate Litzenburger, Kenna Shaw, Jack Lee, Jiexin Zhang, Scott Kopetz. M.D. Anderson Cancer Center, Houston, TX.

Background: The efficacy of small sequencing panels for the initial therapeutic management of patients with solid tumor malignancies is established, especially for melanoma, colorectal cancer, and lung cancer. The utility of such panels for identifying therapeutic targets after front-line therapies have failed is less clear. We completed a clinical trial for the systematic identification of potential therapeutic targets in patients with advanced solid tumor malignancies. A two-staged molecular diagnostics approach was used in which the patients were initially evaluated with a 50 gene next-generation sequencing (NGS) panel that analyzes for hot spot mutations. If no therapeutic targets were identified, or if the patient suffered recurrence following an initial targeted therapy, an NGS panel of 409 full exomes (CMS400) was employed.

Design: Eligibility for the CMS400 panel included completion of standard front-line therapy, performance status of 0 or 1, and being agreeable to participation in a clinical trial if a possible therapeutic target was identified. All NGS was performed on formalin-fixed, paraffin-embedded tumors. Actionable gene was defined as a gene that that can be therapeutically targeted in a matched genotype selected clinical trial. Bioinformatics-based decision support helped to identify if specific gene alterations were activating or variants of uncertain significance.

Results: 42% (217/521) of patients had at least one alteration in an actionable gene identified by CMS400 that was not identified in the initial smaller NGS screen. 182/217 (84%) of the alterations were mutations, and 35/217 (16%) were amplifications. Bioinformatics revealed that 47% of these alterations could be therapeutically targeted. The functional significance of the remaining alterations is currently unknown. 40/217 (18%) patients were subsequently enrolled onto a matched targeted therapy trial. Placement onto such matched trials was associated with significantly improved overall survival after multi-variate analysis.

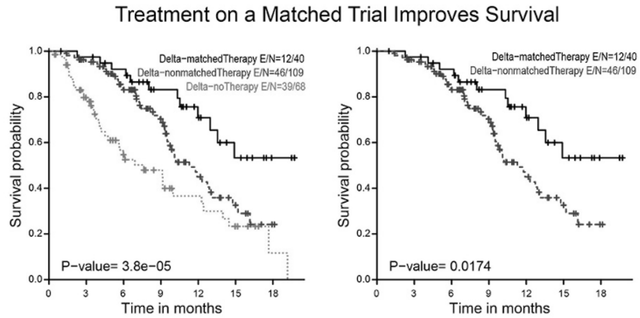

Conclusions: Expanded NGS testing does provide clinical benefit, identifying more patients who are potentially eligible for targeted therapy trials. This is important, as patients treated with this approach have significantly improved survival compared to patients treated on non-matched trials.

1825 Role of Silencer-of-Death- Domain (SODD) in Barrett's Associated Esophageal Adenocarcinoma

Weibiao Cao, Dan Li, Jie Hong. Rhode Island Hospital and the Warren Alpert Medical School of Brown University, Providence, RI; Shanghai Jiao-Tong University School of Medicine Renji Hospital, Shanghai, China.

Background: We have shown that NADPH oxidase NOX5-S may contribute to the progression from Barrett's esophagus (BE) to esophageal adenocarcinoma (EA) via increasing cell proliferation, decreasing cell apoptosis and causing DNA damage. However, the mechanisms of NOX5-S-dependent decrease in cell apoptosis are not fully understood. In this study we examined the role of silencer of death domain (SODD) in NOX5-S-mediated decease in cell apoptosis.

Design: SODD protein expression was determined by Western blot analysis and immunohistochemical staining. Cell apoptosis was examined by caspase-9 activity and an ELISA assay for cell apoptosis. An NF-kB binding element in the SODD promoter was determined by CHIP assay and a gel mobility shift assay.

Results: SODD was significantly increased in EA tissues, EA cell lines FLO and OE33, and a dysplastic cell line CP-B. Strong SODD immunostaining was significantly higher in low-grade dysplasia (66.7%), high-grade dysplasia (81.2%) and EA (71.2%) than in Barrett's mucosa (10.5%). Acid treatment significantly increased SODD protein and mRNA expression and promoter activity in FLO cells, an increase which was significantly decreased by the knockdown of NOX5-S and NF-kB1 p50 with their siRNAs. Overexpression of NOX5-S significantly increased SODD protein expression in FLO cells. Moreover, overexpression of NOX5-S or p50 significantly increased the SODD promoter activity and decreased the caspase 9 activity or apoptosis. NOX5-S overexpression-induced increase in SODD promoter activity was significantly decreased by knockdown of p50. In addition, acid treatment significantly decreased the caspase 9 activity, a decrease which was significantly inhibited by knockdown of SODD. Furthermore, an NF-kB binding element GGGGACACCCT was identified in the SODD promoter.

Conclusions: Acid-induced increase in SODD expression and decrease in cell apoptosis may depend on the activation of NOX5-S and NF-kB1 p50 in FLO cells. It is possible that acid reflux present in patients with Barrett's esophagus may activate NOX5-S. High levels of reactive oxygen species derived from NOX5-S may activate NF-kB1 p50 and upregulate SODD, which in turn decreases cell apoptosis, thereby contributing to the progression from BE to EA.

1826 Expression of GRP78 Protein Is Increased in Pancreatic Ductal Adenocarcinoma and Intraductal Papillary Mucinous Neoplasm

Hannah H Chen, Hui Zhang, Neelima Valluru, Austin McHenry, Stefan Pambuccian, Xianzhong Ding. Loyola University Medical Center, Maywood, IL.

Background: The poor prognosis of pancreatic ductal adenocarcinoma (PDAC) is associated with late detection, aggressive tumor biology and chemotherapeutic resistance. According to the Response Evaluation Criteria in Solid Tumors (RECIST), for pancreatic cancer patients treated palliatively with gemcitabine and nab-paclitaxel, no complete responses were observed, and partial response was only observed in 37% of patients, and progressive disease in 22% of patients. GRP78 is a major endoplasmic reticulum (ER) chaperone protein critical for protein quality control of ER. It is found that GRP78 is preferably required for cancer cell survival, promotes tumor progression and enhances drug resistance. The study aims to explore whether the expression of GRP78 protein in PDAC and intraductal papillary mucinous neoplasm (IPMN) is increased compared to the normal pancreatic ducts using immunohistochemical (IHC) staining method.

Design: The expression of GRP78 were assessed using IHC in 45 cases of formalin-fixed paraffin-embedded tissues, in which normal ducts (38), low grade IPMN (IPMN-LG, 26), high grade IPMN (IPMN-HG, 9), and PDAC (20) were examined. Immunostaining intensity of GRP78 protein was categorized as no or weak staining (0-1+) and strong staining (2-3+). Fisher's exact test with two tails was performed using the GraphPad statistical software.

Results: GRP78 expression was identified in cytoplasm of normal pancreatic ducts, IPMN and PDCA with a fine granular pattern. All PDAC and IPMN-HG show strong

expression of GRP78 while the normal ductal cells show only minimal expression of GRP78. 73% of IPMN-LG expresses GRP78 strongly. Statistical analysis revealed significant difference in GRP78 expression levels between normal ductal cells and all three pathological conditions including PDCA, IPMN-HG and IPMN-LG (all p<0.0001).

	Normal pancreatic ducts	IPMN-LG	IPMN-HG	PDAC
Total	38	26	9	20
No or weak staining (0-1+)	37	7	0	0
Strong staining (2-3+)	1	19	9	20
% of strong staining	3%	73%	100%	100%

Conclusions: This study shows that the expression levels of GRP78 are significantly increased in PDAC, IPMN-HG and IPMN-LG compared to the normal pancreatic ductal cells. It appears that there is a progressive increase in GRP78 expression from IPMN-LG to IPMN-HG and invasive ductal carcinoma. Increased GRP78 expression may contribute poor responsiveness of PDCA to conventional chemotherapy.

1827 MicroRNA Profiling to Identify Racial Disparities in Smoking Related Lung Tumorigenesis

Jinjun Cheng, Chuanhe Yang, Wafi Bibars, Meiyun Fan, Benny Weksler, Lawrence Pfeffer. The University of Tennessee Health Science Center, Memphis, TN.

Background: African Americans (AA) have higher incidence of lung cancer, and higher mortality compared to other racial groups, in particular Caucasians (C) in the United States. However, the underlying mechanism is unclear. MicroRNA profiling has been used to identify molecular mechanisms of tumorigenesis, predict patient prognosis, and study cancer in specific populations. This study was designed to explore differences in microRNA expression between AA and (C) lung cancer patients.

Design: This is a retrospective analysis of stage I lung cancer patients treated at Methodist University Hospital (MUH) during last 10 years. AA and C were matched according to smoking history, age, gender, histological type, and grade. Lung tumor specimens from AA and Caucasian were compared. RNA was extracted from 12 pairs of formalin-fixed paraffin-embedded tissue blocks of smoking associated primary lung squamous cell carcinoma in AA and Caucasians. Changes in microRNA expression were explored by Nanostring miRNA expression assay. Statistical analyses were performed using Graphpad Prism. To further validate our data, we reanalyzed microRNA expression data from a large cohort of lung squamous cell carcinoma patients as part of The Cancer Genome Atlas (TCGA) project.

Results: We matched 12 pairs of patients with squamous cell carcinoma. There was no statistically significant difference in patient gender, histology type, grade and death rate between AA and C patients, but AA were slightly older (69.6 years vs. 65.2 years, p =0.049). In comparing the two groups of tumor samples, 6 microRNAs were significantly associated with race. Notably, miR-200b-3p (p =0.016), miR-200a-3p (p=0.029), and miR-4286 (p =0.049) were slightly but statistical significantly upregulated in AA lung tumor tissue, while miR-142-3p (p =0.007), miR-135b-5p (p =0.019), and miR-29b-3p (p =0.011) were significantly downregulated.

Conclusions: Based on miRNA expression patterns in different subtypes of lung squamous cell carcinomas (*i.e.*, primitive, classical, secretory and basal) in the TCGA database, our results suggest that tumor tissue from AA-patients have a miRNA expression signature characteristic of primitive tumors that are known to be associated with more aggressive tumor biology and poor prognosis. Further analysis of larger sample of lung cancer is needed to validate our findings.

1828 Platelet Cloaked Tumour Cells Educate M2 Macrophage Differentiation

Chris Cluxton, Cathy Spillane, Mark Ward, Cara M Martin, Orla Sheils, Frederick Sheedy, Sharon O'Toole, John J O'Leary. Trinity College Dublin, Dublin, Ireland; The Coombe Women & Infants University Hospital, Dublin, Ireland.

Background: During the metastatic cascade, circulating tumour cells rapidly and efficiently adopt a platelet cloak. Platelet cloaking of tumour cells promotes metastatic disease by promoting cellular proliferation, angiogenesis and EMT while inhibiting autophagy and apoptosis. The aim of this study is to examine the role of platelets in promoting macrophage education towards an M2 tumour sparing phenotype.

Design: Enriched PBMCs from buffypacks were harvested and purified by plastic adhesion in the presence of human serum (10%). Monocytes were stimulated for 24hours with RPMI media supplemented with supernatant from ovarian (59M and SKOV3) and breast (MCF-7) cell lines that were either uncloaked or cloaked with washed platelets from healthy donors. The protocol was repeated with live tumour cells in transwells for 48hours. Cytokine stimulations with IFNy/LPS (10ng/mL each) or IL10/TGFbeta (50ng/mL,20ng/mL) were included as experimental controls for M1 and M2 education, respectively. Messenger RNA for the M1 cytokine TNFalpha, the pleiotrophic cytokine IL-6, and the M2 molecules IL-10, fibronectin-1, VEGF and TGFbeta was measured to quantify M1/M2 education.

Results: We firstly demonstrated that monocytes isolated using our protocol could be induced to differentiate into M1 and M2 macrophages by their respective stimulatory cytokines. We then confirmed that for both experimental designs, the supernatants from naturally de-granulated platelets in the absence of tumour cells and platelet cloaked tumour cells suppressed the transcription of TNFalpha and induced IL-10, IL-6, FN-1, VEGF and TGFbeta supporting the hypothesis of monocyte education to M2 macrophages compared with tumour cells lacking the platelet cloak.

Conclusions: Platelet cloaked tumour cells induce education of monocytes towards the tumour sparing M2 phenotype. These cells release immune suppressive molecules that may contribute to tumour cell immune evasion during the metastatic cascade.

1829 Discordant Expression of cMYC and PD-L1 in Various Human Tumors

Jarish Cohen, Sarah Bowman, Gyula Szabo, Sarah E Umetsu, Gregor Krings, Zoltan Laszik. University of California, San Francisco, San Francisco, CA.

Background: The PD-1/PD-L1 co-inhibitory pathway is a major target of cancer immunotherapy. In addition to being upregulated in response to inflammatory stimuli, PD-L1 can be expressed by intrinsic oncogenic signaling pathways. Recently, increased cMyc oncoprotein expression was shown to increase PD-L1 mRNA and protein in vitro through occupancy of the PD-L1 promoter. cMyc is overexpressed in a variety of human tumors and can be associated with a poor prognosis. Although cMyc overexpression was shown to correlate with PD-L1 mRNA expression in certain human tumors, the association of PD-L1 and cMyc protein expression in primary human tumor tissue has not been investigated.

Design: cMYC and PD-L1/CD8 (dual stain) immunohistochemistry was performed on consecutive breast carcinoma (154 cases), prostatic adenocarcinoma (34 cases), renal cell carcinoma (RCC, 62 cases), and hepatocellular carcinoma (HCC, 66 cases) tumor tissue microarray serial sections. Whole slide digital images were generated and analysis of cMYC and PD-L1 expression as well as the CD8 T cell infiltrate was performed using Definiens digital image analysis software. cMYC positive cases were defined as having greater than 10% intermediate and high expressing cells of total cMYC positive cells. PD-L1 positive cases were those in which any positive PD-L1 expression was observed.

Results: Positive cMYC and PD-L1 expression was observed in a small subset of cases across all tumor types (Table 1). In cases that had positive cMYC expression, a correlation with PD-L1 expression was not seen. Within breast carcinoma cases, positive cMYC and PD-L1 expression trended toward triple negative (ER-/PR-/HER2-) tumors. In addition, PD-L1 expression demonstrated significant correlation with CD8 T cell infiltration in the HCC (p=0.002) and breast carcinoma cases (p=0.05).

	HCC	Breast Carcinoma	Prostatic Adenocarcinoma	RCC
cMYC+	6/66 (9%)	21/154 (14%)	8/34 (24%)	14/62 (23%)
PD-L1+	11/66 (17%)	9/154 (6%)	0/34 (0%)	3/62 (5%)

Conclusions: A small percentage of HCC, RCC, breast carcinoma, and prostatic adenocarcinoma cases demonstrate increased cMYC and PD-L1 expression. However, PD-L1 protein expression does not significantly correlate with cMYC expression by immunohistochemistry. PD-L1 and cMYC tended to be more highly expressed by a breast cancer subtype that is associated with a poorer prognosis. A subset of tumors demonstrates high PD-L1 expression in the context of increased CD8 T cell infiltration and might represent an adaptive resistance mechanism to the anti-tumor immune response.

1830 Which *PTEN* Alterations Are Associated with Protein Loss?

Suzanne Crumley, Russell R Broaddus. The University of Texas M.D. Anderson Cancer Center, Houston, TX.

Background: *PTEN* is an important tumor suppressor and is thus a component of many multi-gene next-generation sequencing (NGS) panels. Mutation may result in loss of *PTEN* protein expression, resulting in PI3K–AKT pathway activation and providing a potential therapeutic target. It is not known how often mutation results in protein loss. Our goal was to define the specific mutations in *PTEN* identified in a clinical setting and determine how these impact protein expression.

Design: Clinical NGS was performed on 1,192 patient tumors using 46, 50, or 409 multi-gene panels. PTEN IHC was performed in a subset. 161 *PTEN* mutations were identified in 137 patients. 21 patients had multiple *PTEN* mutations. The 117 cases with both a *PTEN* mutation and IHC were reviewed for associations between mutation type, IHC result, and primary site.

Results: The majority of *PTEN* mutant tumors were of Müllerian (76/117) or brain (19/117) origin, as well as a variety of other sites. Overall, 56 (48%) of *PTEN* mutant tumors had loss of PTEN IHC expression. Nonsense mutations most commonly resulted in PTEN protein loss, but 27% of these had retained expression. Depending on histology, nearly a third of missense mutations and half of the splice site mutations were associated with PTEN protein loss. Protein loss was uncommon in *PTEN* mutant brain tumors compared to the other tumor types. Amongst the nonsense mutations, the most frequent alteration resulting in protein loss was a single nucleotide variant (SNV). Deletion size was smaller in cases with retained PTEN expression.

Table 1. Classes of *PTEN* Mutations

	PTEN Expression Intact (n; % of mutations in tumors with positive IHC expression)	PTEN Expression Lost (n; % of mutations in tumors with negative IHC expression)	Total Mutations
Mullerian Primary			
Nonsense	6 (14%)	31 (60%)	37
Missense	34 (77%)	16 (31%)	50
Splice	3 (7%)	3 (6%)	6
NOS	1 (2%)	2 (4%)	3
Total Mutations	44	52	96
Brain			
Nonsense	4 (22%)	0	4
Missense	12 (67%)	0	12
Splice	2 (11%)	1 (100%)	3
NOS	0	0	0
Total Mutations	18	1	19
Other tumor types			
Nonsense	4 (36%)	7 (64%)	11
Missense	4 (36%)	1 (9%)	5
Splice	3 (27%)	3 (27%)	6
NOS	0	0	0
Total Mutations	11	11	22

Table 2. Classification of Nonsense Mutations

	PTEN Expression Intact (n; % of mutations in tumors with positive IHC expression)	PTEN Expression Lost (n; % of mutations in tumors with negative IHC expression)	Total Mutations
Deletion # bp lost	8 (57%) median 2, mean 4.4, range 1-17	15 (39%) median 4, mean 9.4, range 1-97	23
SNV	2 (14%)	18 (47%)	20
Duplication	3 (21%)	5 (13%)	8
Insertion	1 (7%)	0	1
Total Mutations	14	38	52

Conclusions: Nonsense mutations are more frequently associated with PTEN protein loss and missense mutations with PTEN protein retention. However, gene alteration does not accurately predict protein loss. Therefore, we recommend that IHC be used to follow-up on *PTEN* mutations detected in clinical NGS panels. Bioinformatics can help predict which mutant tumors with intact protein expression are potentially expressing non-functional protein.

1831 Genomic Landscape and Clinical Features of Carcinomas with ERBB2 S310 Extracellular Domain Mutations

Patrice Desmeules, Ahmet Zehir, David M Hyman, Maria E Arcila, Marc Ladanyi. Memorial Sloan Kettering Cancer Center, New York, NY.

Background: Alterations in human epidermal growth factor receptor 2 (HER2/ERBB2) have been identified as potential therapeutic targets in several cancer types. While amplification/overexpression and mutations within the tyrosine kinase domain (KD) of ERBB2 have been the main focus of therapeutic approaches, mutations in the extracellular domain (ECD) are becoming increasingly recognized as distinct and potentially targetable oncogenic drivers. S310F and S310Y are by far the most frequent mutations located in ECD. They result in increased kinase activity from C-terminal tail hyperphosphorylation and emerging evidence supports the efficacy of ERBB2 inhibitors against this type of alteration. We aimed to characterize the profile of these mutations in a large dataset of tumors that underwent comprehensive genomic profiling.
Design: Tumor and matched germline DNA for each patient were processed through a hybridization capture-based next-generation sequencing assay for targeted deep sequencing of 410 key cancer genes. Genomic and clinicopathological data in tumors harboring ERBB2 S310 mutations were collected.
Results: Sixty-seven patients with tumors harboring a S310F/Y mutation were identified in 16 different tumor sub-types, with a median age of 66 and male predominance. These alterations represented 74% of ECD mutations in the matched tumor types and were predominantly seen in urothelial (UC; 45%) and breast (15%) carcinomas. Fifteen concurrent mutations were identified on average, not differing between tumor types ($p = 0.09$). Only a few S310 mutated tumors (9%) had another driver mutation (BRAF, EGFR or KRAS), similarly to all tumors with ECD (10%) or KD (16%) alterations combined. Co-amplification of ERBB2 was seen in 40 to 50 % of lung, breast and hepatobiliary carcinomas, while less frequently in colorectal, UC and other carcinomas combined (20%, 13% and 0%, respectively; $p=0.04$). ECD mutations represented the majority of ERBB2-altered UC (63%), in contrast to breast and lung tumors, where KD alterations were dominant (66 and 68%, mostly L755P and exon 20 insertions). Amongst this cohort, thirteen patients (19%) with S310 mutated tumors at advanced stage were eligible to receive a form of ERBB2 /EGFR inhibitor.
Conclusions: Comprehensive genomic profiling of tumors reveals that ERBB2 S310 mutations are not rare, frequently distinct from amplification and encountered in a wide range of tumor types. Identification of these variants may allow a significant number of patients to be considered for ERBB2 /EGFR inhibitor therapy.

1832 Immune Check-Point Blockade as a Potential Therapeutic Strategy for Undifferentiated Malignancies

Kelly Devereaux, Gregory Charville, Shuchun Zhao, Athena Cherry, Matt van de Rijn, Yasodha Natkunam. Stanford Health Care, Stanford, CA.

Background: Undifferentiated malignancies (UMs) pose a therapeutic challenge. Given that the cell of origin is unknown, this class of tumors is largely empirically treated with nonspecific chemotherapeutic agents that yield poor clinical response. Immunotherapy-based targeting of the programmed cell death 1 (PD-1) or its ligands (PD-L1 and PD-L2) to promote anti-tumor T-cell activity has emerged as a promising method to effectively treat a diverse set of cancers, particularly those with a higher-mutational burden secondary to genomic instability. Although UMs encompass a diverse set of neoplasms, they share an aggressive, genetically unstable pathobiology that we predict will be particularly amenable to checkpoint inhibitor therapy.
Design: Formalin-fixed, paraffin-embedded (FFPE) tissue sections from UMs, including undifferentiated carcinomas (15 cases), undifferentiated malignant neoplasms (15 cases) and undifferentiated pleomorphic sarcomas (62 cases), from indiscriminate anatomic locations were selected. Immunohistochemistry for PD-1 ligands (PD-L1 and PD-L2) was performed and the average intensity of staining (negative, weak, strong) is reported.
Results: Of the cohort of UMs, PD-L1 was expressed in the majority of undifferentiated carcinomas (67%) and undifferentiated malignant neoplasms (73%) (Table 1). Although fewer undifferentiated pleomorphic sarcomas expressed PD-L1 (13%), the majority (76%) showed expression of PD-L2.

Table 1. Expression of PD-L1 in undifferentiated malignancies

PD-L1 expression	Undifferentiated carcinoma	Undifferentiated malignant neoplasm	Undifferentiated pleomorphic sarcoma
Positive	10 (67%) (8 strong, 2 weak)	11 (73%) (5 strong, 6 weak)	8 (13%) (4 strong, 4 weak)
Negative	5 (33%)	4 (27%)	54 (87%)

Conclusions: Here we show that UMs have aberrant, increased expression of PD-L1 or PD-L2 in a high proportion (>50%) of tumors, suggesting this heterogeneous class of tumors share a common pathobiology of immune check-point dysregulation. *9p24.1* FISH analysis to assess for chromosomal alterations at this locus, which harbors the *PD-L1* and *PD-L2* genes, will be important to determine a genetic basis for PD-L1/PD-L2- mediated tumor immune evasion. The findings of this study provide provisional molecular data and support for using checkpoint inhibitors as a novel treatment approach and has the potential to change management and disease outcome in patients with UMs.

1833 Stem Cell Features and Accumulation of Genetic Alterations Define Anaplastic Thyroid Carcinomas

Salvador Diaz-Cano, Juan Gonzalez, Hiba ElHassan, Alfredo Blanes. King's College Hospital, London, United Kingdom; University of Malaga School of Medicine, Malaga, Spain.

Background: Stem cell features and genetic definition of tumor grade is not available for follicular cell derived thyroid carcinomas. We aim to assess whole exome sequencing and stem cell markers in high-stage high-grade thyroid carcinomas.
Design: We selected stage IV thyroid carcinomas (TC): widely invasive follicular (WI-FTC, 15), papillary (PTC, 21), poorly differentiated thyroid carcinoma (PDTC, 19), and anaplastic carcinomas (ATC, 14 with differentiated component and 15 without). Whole-exome sequencing was performed on tumor and normal tissue samples, using a Random Forest machine learning approach to compare ATC with and without differentiated component, and differentiated part vs. stage IV differentiated TC vs. PDTC. Predictive Model Analysis Pipeline and Methods ► Functional somatic mutations unique to tumors were identified and represented as a samples x genes mutation matrix (mutated=1, non-mutated=0). ► Pairwise Random Forest models were built for each diagnostic category ► Variable selection was conducted using Fisher's Exact test with 5x10 fold cross-validation design. Random Forest models were based on the training set using the caret package in R, and predictive accuracy measured in an independent test set. Telomerase immunostaining and FISH-PNA of telomere were also analyzed.
Results: The grade-predictive genes included ARID1A (P=2.46E-09), MAPK10 (P=4.35E-08), CTNNB1 (P=3.19E-16), PIK3CA (P=2.12E-07), PIK3R1 (P=1.67E-11), PTEN (P=5.19E-25), and TP53 (P=8.65E-45). ATC–PDTC distinction was mainly dependent on the average number of target mutated genes (7 vs. 3), with no significant differences between ATC differentiated component and stage IV differentiated TC. Telomerase was significantly higher in PDTC-ATC ($p<0.001$), correlating with PNA-FISH detectable telomeres. PNA-FISH detectable telomere in more than 20% tumor cells was observed in high-grade lesions (PDTC-ATC), in particular at tumor periphery.
Conclusions: Stem cell features and accumulation of cooperative genetic mutations defined poorly differentiated thyroid carcinomas. Maintained stem cell features in peripheral tumor cells would contribute to higher metastatic potential.

1834 Profiling Toll-Like Receptor Pathway Mutations and Expression in Esophageal Adenocarcinoma

Daffolyn R Fels Elliott, Juliane Perner, Martyn F Symmons, Brett Verstak, Xiaodun Li, Maria O'Donovan, Nick J Gay, Rebecca C Fitzgerald. University of Cambridge, Cambridge, United Kingdom; Cambridge University Hospital NHS Trust, Cambridge, United Kingdom.

Background: Altered innate immune signaling may disrupt host-microbe homeostasis and promote an inflammatory microenvironment that favors tumorigenesis. We aimed to determine whether mutations in esophageal adenocarcinoma (EAC) could affect Toll-like receptor (TLR) pathway genes and alter TLR signaling.
Design: The mutational profiles of TLR pathway genes were interrogated using whole genome sequencing from 172 EAC patients with clinical outcome data and 24 adjacent Barrett's esophagus samples. PathScan software was used to analyze the significance of mutations collectively affecting the TLR pathway. Immunohistochemistry was performed with TLR4 monoclonal antibody on FFPE tissue microarrays to investigate TLR4 expression in non-dysplastic Barrett's esophagus (n=66), low grade dysplasia (n=17), high grade dysplasia (n=29) and EAC (n=335), in triplicate. To determine the functional relevance of *TLR4* mutations, site-directed mutagenesis and luciferase reporter gene assays were carried out in HEK293 cells.
Results: TLR pathway genes were mutated in 23/172 (13%, $p=5.1\times10^{-6}$) of EAC tumors and rarely mutated in adjacent Barrett's. Tumors with TLR pathway mutations had more advanced disease stage and metastasis ($p=0.029$), but there was no difference in median survival ($p=0.355$). *TLR4* was the most frequently mutated gene with nine mutations in 8/172 (5%) tumors, all of which were verified using Sanger sequencing. At the protein level TLR4 was over-expressed in EAC compared to Barrett's and dysplasia ($p<0.0001$). The *TLR4* mutants E439G, S570I, F703C and R787H were confirmed to have impaired reactivity to bacterial lipopolysaccharide with marked reductions in signaling by luciferase reporter assays. *TLR4* mutations were also detected in external datasets including 22/563 (3.9%) of gastric adenocarcinoma, 53/811 (6.5%) of lung adenocarcinoma and 42/806 (5.2%) of melanoma samples, suggesting that our findings may be relevant to other cancers that are exposed to microbial communities.
Conclusions: TLR pathway genes are recurrently mutated in EAC and linked with more advanced disease stage. *TLR4* mutations have decreased responsiveness to bacterial lipopolysaccharide and may play a role in the pathogenesis of this disease.

1835 Use of Core Needle Biopsies for Molecular Characterization of Advanced Pancreatic Ductal Adenocarcinoma (PDAC) – The COMPASS Trial

Sandra Fischer, Kyaw Aung, Rob E Denroche, GunHo Jang, Faiyaz Notta, Sangeet Ghai, Julie M Wilson, Anna J Dodd, Sheng-Ben Liang, Dianne Chadwick, Neesha Dhani, David Hedley, Jennifer J Knox, Steven Gallinger. University Health Network, Toronto, ON, Canada; Ontario Cancer Institute for Cancer Research, Toronto, ON, Canada.

Background: As knowledge of the genomic landscape of PDAC expands, there is hope that molecular profiling can identify subgroups of patients for better treatment selection. The use of needle biopsies for genomic studies is safe with a small risk of complications; however inadequate samples (e.g. insufficient tissue, necrotic and non-representative biopsies) can significantly impact the ability to obtain deep molecular profiling data. Feasibility results of an ongoing prospective study involving comprehensive molecular characterization of advanced PDAC are shown.

Design: Through the UHN/OICR PanCuRx Translational Research Initiative COMPASS trial (NCT – 02750657), patients with advanced PDAC undergo image guided 18G-needle biopsies for whole genome (WGS) and transcriptome sequencing (WTS). Fresh cores are snap-frozen in OCT, and sections are cut to select the most suitable cores for laser capture microdissection (LCM). Tumor samples undergo DNA and RNA extraction for WGS and WTS, respectively. Whole blood samples are collected at baseline for WGS of germline DNA. WGS and WTS are performed using next generation sequencing with minimum target depth of coverage at 45X for tumor and 30X for reference.

Results: Since December 2015, 29 patients have contributed tumor samples for genomic profiling. Liver was the most frequent biopsy site (23/29). DNA and RNA quality was satisfactory for WGS and WTS in 96% (25/26) and 88% (23/26) cases, respectively. On average tumor cellularity after LCM was 73% (cut off for WGS >20%). 3-6 (average 3.7) cores were obtained from each patient, with an aggregate core length per case of 1.6-5.6 cm (average 3.0 cm). 1-4 cores were used for LCM per case (average 2 cores). The average viable tumor content per case was 61%.

Conclusions: Fresh tissue cores obtained through image assisted needle biopsies can produce high quality material for genomic profiling of advanced PDAC with the aim to identify candidates eligible for personalized treatment.

1836 Mutations in *TSC1* and *TSC2* Are Associated with High Tumor Mutational Burden and Therapeutic Options

Laurie M Gay, Julia A Elvin, James Suh, Jo-Anne Vergilio, Shakti H Ramkissoon, Alexa Schrock, Siraj M Ali, David Fabrizio, Garrett Frampton, Vincent Miller, Philip Stephens, Jeffrey Ross. Foundation Medicine, Inc., Cambridge, MA; Albany Medical College, Albany, NY.

Background: *TSC1* and *TSC2* regulate the MTOR pathway, and loss of *TSC1/2* are linked to sensitivity to MTOR inhibitors. We analyzed 85,866 clinical samples by comprehensive genomic profiling (CGP) to determine the frequencies of *TSC1/2* genomic alterations (GA) and corresponding tumor mutational burden (TMB).

Design: DNA (≥50ng) was extracted from 85,866 tumor specimens. CGP was performed on hybridization-captured, adaptor ligation-based libraries (mean coverage depth >550X) for up to 315 cancer-related genes plus select introns from 28 genes commonly rearranged in cancer. TMB (mut/Mb) was calculated over 1.1 Mb by counting somatic, non-driver GA. GA included base substitutions, INDELs, copy number changes, and rearrangements.

Results: 771 (0.9%) cases had *TSC1* GA; 828 (1.0%) had *TSC2* GA. *TSC1* GA were enriched in urothelial carcinomas (CA) [bladder (UCB, 7.8%), kidney (11.4%), and unknown primary (UP)(10.3%)] and other kidney CA [clear cell (7.2%) and NOS (4.5%)]. *TSC1* GA are also common in osteosarcoma (2.8%), medulloblastoma (2.8%), uterine leiomyosarcoma (2.5%), endometrial adenocarcinoma (2.4%), and hepatocellular carcinoma (HCC, 1.9%). In addition to angiomyolipoma (60%) and PEComa (35.5%), *TSC2* GA were enriched in pancreatic neuroendocrine CA (8.8%), HCC (4.7%), ovarian carcinosarcoma (3.9%), soft tissue sarcomas (3%), neuroendocrine CA of UP (2.1%), and ovarian/fallopian/peritoneal serous CA (1.8-2.3%). 0.6-1.3% of common tumors - NSCLC, invasive ductal breast CA (IDC), GBM, and CRC - harbor *TSC1/2* GA, representing a significant number of patients whose tumors may respond to mTOR inhibitors. Cases with *TSC1/2* GA commonly have high TMB, as seen for 5 common tumor types. All tumors with high levels of microsatellite instability (MSI) and *TSC1/2* GA had high TMB; 12% of MSI-stable, *TSC1/2*-mutated tumors had high TMB. Responses to MTOR-targeted therapies and checkpoint inhibitors (ICPI) will be presented.

Conclusions: *TSC1/2* GA occur in many tumor types, are often identified in cases with high TMB, and are associated with responses to therapies targeting the MTOR pathway or ICPI in cases with high TMB.

	NSCLC	UCB	IDC	CRC	DLBCL
Total cases	15,366	1,129	10,336	8,186	341
TSC1 GA	0.7%	7.8%	0.6%	0.6%	0.3%
TSC1 mutated, TMB ≥10	49%	44%	20%	52%	100%
TSC2 GA	0.9%	0.6%	0.8%	0.8%	0.9%
TSC2 mutated, TMB ≥10	54%	38%	26%	26%	100%

1837 Pan-TRK IHC Is an Efficient and Reliable Screening Assay for Targetable NTRK Fusions

Jaclyn F Hechtman, Alexander Drilon, David M Hyman, Ahmet Zehir, Snjezana Dogan, Maria E Arcila, Marc Ladanyi, Ryma Benayed, Achim Jungbluth. Memorial Sloan Kettering Cancer Center, New York, NY.

Background: Activating neurotrophic tyrosine receptor kinase (NTRK) fusions are typically detected via DNA or RNA based assays and are highly targetable with new NTRK inhibitors. Here, we explore the sensitivity of pan-TRK immunohistochemistry (IHC) for the detection of activating NTRK fusions.

Design: NTRK fusions were detected prospectively by clinical genomic profiling of patients with advanced cancer using MSK-IMPACT, a DNA-based next generation sequencing assay. Novel NTRK rearrangements detected on MSK-IMPACT were further characterized at the RNA level for evidence of transcription via Archer Dx fusion assay. Expression of NTRK-1, -2, and -3 was detected via IHC with anti- pan-NTRK mAb EPR17341 (Abcam, 1:250) and performed on all cases with NTRK rearrangements.

Results: Of 10 cases (*NTRK1*: n=6, *NTRK2*=1, *NTRK3*: n=3) with rearrangements, 7 were known activating fusions in the literature while 3 were novel and of unknown functional significance. Archer detected a fusion transcript in 1 of 3 cases with novel DNA level NTRK rearrangements. 7 of 10 cases with DNA level rearrangements were positive by pan-TRK IHC, including the novel rearrangement verified by Archer. The 3 IHC-negative cases included 2 novel DNA level NTRK rearrangements (*ZNF710-NTRK3* and *NTRK1- P2RY8*), neither of which were transcribed via Archer and 1 mismatch repair- deficient colorectal carcinoma with an *ETV6-NTRK3* fusion. Pan-Trk IHC sensitivity for transcribed NTRK fusions was 88% while both cases with non-transcribed, DNA level NTRK rearrangements were negative on IHC. Pan-TRK IHC was consistently negative in internal controls such as non-neoplastic lymphocytes, hepatocytes, colorectal epithelium, alveolar epithelium, and renal cortex. All IHC positive cases had cytoplasmic staining. Interestingly, both *LMNA1-NTRK1* fusions displayed nuclear membrane staining while both *TPM3* fusions showed cellular membrane staining.

Conclusions: Pan-Trk IHC is a time- and tissue-efficient screen for NTRK fusions with high sensitivity. IHC is helpful in predicting functionality of novel NTRK rearrangements by confirming that they are productive and may also predict possible fusion partners based on staining patterns. IHC detection of pan-TRK should be included in the molecular work-up of candidates for NTRK inhibitor therapy.

TUMOR TYPE	PARTNER GENE	NTRK GENE	STAINING PATTERN				ARCHER
			CYTOPLASMIC	PERI-NUCLEAR	MEMBRANOUS	NUCLEAR	
GLIOBLASTOMA	AFAP1	NTRK1	X	X	X		POSITIVE
COLORECTAL CARCINOMA	LMNA	NTRK1	X	X			N/A
SARCOMA	LMNA	NTRK1	X	X			POSITIVE
LUNG ADENOCARCINOMA	P2RY8	NTRK1					NEGATIVE
COLORECTAL CARCINOMA	TPM3	NTRK1	X		X		N/A
LUNG ADENOCARCINOMA	TPM3	NTRK1	X		X		POSITIVE
COLORECTAL CARCINOMA	ETV6	NTRK3					N/A
MAMMORY ANALOGUE SECRETORY CARCINOMA	ETV6	NTRK3	X				N/A
GLIOBLASTOMA	ZNF710	NTRK3					NEGATIVE
GLIOBLASTOMA	BCR	NTRK2	X				POSITIVE

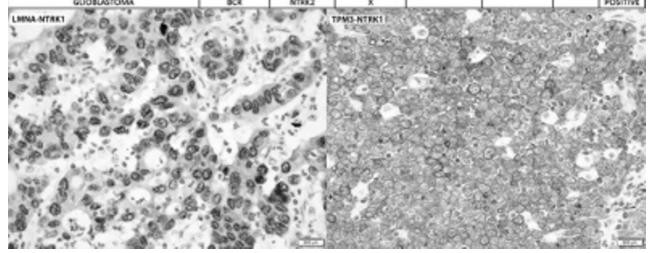

1838 Expression of Zinc Transporter ZIP6 (LIV-1) in Colon Carcinoma

Mobashir Hosameddin, Rami Hayajneh, Andre Kajdacsy-Balla, Grace Guzman, Virgilia Macias. University of Illinois at Chicago, Chicago, IL.

Background: Zinc is an essential metal for several cell functions. The ZIP family (Zrt-, Irt-like protein) facilitates the uptake of zinc into the cytosol. The ubiquitous zinc transporter ZIP6 (LIV-1 subfamily) has been implicated in epithelial-mesenchymal transition, cell migration, anoikis resistance and invasive behavior in human tumors. Elevated expression is seen especially in tissues sensitive to steroid hormones. To date, studies addressing ZIP6 expression in intestinal tumors have not been published. Our aim was to characterize its expression in colon cancer by immunohistochemistry and compare it with that of normal colon mucosa.

Design: The expression of ZIP6 in human colorectal cancer was explored using the Oncomine database mining tool. The search revealed overexpression of ZIP6 in colorectal cancer compared to normal tissue. For the study, a tissue microarray (TMA) with duplicates of carcinoma and normal mucosa from 130 patients who underwent colectomy for colon cancer was used. We were able to compare expression in both compartments in 88 patients. TMA slides were incubated with rabbit polyclonal anti-human SLC39A6 antibody (ab61307, 1:100, Abcam) followed by Bond™ polymer refine detection HRP system (Leica Biosystems, DS9800). Cytoplasmic staining was scored semi-quantitatively as follows: 0, negative; 1+, weak; 2+, moderate; and 3+, strong. Percentage of positive epithelial cells were recorded and multiplied by intensity levels to obtain a final immunoreactivity score (IS) for each case. The primary antibody was previously validated in in stable ZIP6 siRNA expressing cell lines. Paired Wilcoxon rank sum test was performed for statistical analysis.

Results: All four databases submitted to data mining showed clearly increased ZIP6 mRNA expression in colon cancer. Diffuse cytoplasmic protein expression was observed in the tumor cells and benign colonic mucosa (mean 2.23 in carcinoma *vs.* 2.33 in normal mucosa); however, the Wilcoxon Test showed no statistically significant differences ($p = 0.126$) between the two compartments.

Conclusions: ZIP6 is known to have wide tissue distribution, including the intestinal tract. It is mainly a cell surface and endoplasmic reticulum protein. Previous studies have shown overexpression in breast, prostate, pancreas, cervix, esophagus and liver cancers. Our study was not able to demonstrate significant differences in ZIP6 expression in a series of colon cancer compared to controls. Since ZIP6 mRNA levels are increased in colorectal cancer in general, it is plausible that post-translational modifications down modulate its protein expression.

1839 CCR10-Expressing IgG+ Plasma Cells Compensate for IgA Deficiency in Colon of Patients with Selective IgA Deficiency

Shaomin Hu, Yanhua Wang, Joseph Albanese, Yungtai Lo, Qiang Liu. Montefiore Medical Center/AECOM, Bronx, NY.

Background: Selective IgA deficiency (sIgAD) is a primary immunodeficiency disease with undetectable serum IgA levels but normal amounts of other types of immunoglobulins. Although IgA is the vastly dominant immunoglobulin in intestines and plays significant roles in intestinal homeostasis, most sIgAD patients are asymptomatic. Compensatory intestinal IgM production was thought to account for lack of clinical symptoms in those patients, while the role of IgG remains unclear. Indeed, increased levels of IgG have been detected in sera of majority sIgAD patients and in intestinal secretions of IgA-/- mice. Furthermore, sIgAD patients are more susceptible to infections in the presence of concomitant deficiency of IgG. All these studies suggest the involvement of IgG in the compensation of intestinal IgA deficiency. Our primary aim in this study is to investigate the composition (IgG+ vs IgM+) of plasma cells in colons of sIgAD patients. As our previous studies showed critical roles of CCR10 in regulating intestinal IgA responses, we are also interested here to explore the expression of CCR10 in compensatory intestinal IgG+ or IgM+ plasma cells.

Design: Colon biopsy specimens from 16 sIgAD patients and 5 control patients (with normal serum IgA levels) were identified, and analyzed for the frequency of IgA+, IgG+ and IgM+ plasma cells and the expression of CCR10 by immunohistochemical stain.

Results: Most of the patients were biopsied for ruling out colon cancer. There was no significant medical history of colitis in any of the patients. Our results showed that there was comparable number of total plasma cells in intestinal mucosa of sIgAD patients to that of control patients. The number of colon mucosal IgA+ plasma cells was 8.2 ± 17.8/high power field (HPF) in the 16 sIgAD patients, compare to 211.0 ± 119.6/HPF in the 5 control patients ($p<0.001$). In contrast, the density of IgG+ plasma cells increased significantly from 6.6 ± 4.8/HPF in control patients to 168.0 ± 79.8/HPF in sIgAD patients ($p<0.001$). The density of IgM+ plasma cells was only slightly increased from 23.0 ± 7.8/HPF to 62.2 ± 74.2/HPF ($p=0.23$) in sIgAD patients. Furthermore, for sIgAD patients, almost all IgG+ and IgM+ plasma cells in colon mucosa express CCR10.

Conclusions: Our results demonstrated that IgG+ plasma cells are the most dominant plasma cells compensating for the IgA deficiency in the colon of sIgAD patients. We also revealed that IgG+ and IgM+ plasma cells in the colon express CCR10, which suggests a regulatory role of CCR10 in the intestinal IgG and IgM responses.

1840 Both MHC I and MHC II Pathways Are Associated with Improved Survival in Triple-Negative Breast Cancer

Jabed Iqbal, Joe Yeong, Bernett Lee, Jeffrey CT Lim, Xin Min Cheng, Puay Hoon Tan. Singapore General Hospital, Singapore, Singapore; A*STAR, Singapore, Singapore.

Background: Triple-negative breast cancer (TNBC) is a heterogeneous subtype with potentially diverse patient outcomes. Approximately 40% of patients experience rapid relapse, while the remaining patients have long-term disease-free survival. Human leukocyte antigen (HLA A,B,C) class I molecules act as antigen-presenting molecules for cytotoxic T lymphocytes (CTLs), which recognize tumor antigens presented on the cell surface with HLA class I molecules, and kill the target cell. HLA class II molecules (HLA-DR and HLA-DQ) are essential for antigen presentation to T-helper lymphocytes, and their expression may be responsible for triggering the immune response.

Design: We examined 323 TNBC samples diagnosed in Singapore general Hospital between 2003 and 2013 using quantitative, digital gene expression NanoString assay to measure expression of a panel of 1199 cancer progression-associated and immune response genes. Various percentiles of gene expression was used as threshold to divide samples into high and low-expressing categories. Genes that were significantly expressed were identified using one-way ANOVA in R version 3.1.2.

Results: Expression of both HLA class I (eg, HLA-A,HLA-B, HLA-C) and HLA class II (HLA-DRA, DRB1,DRB3) genes were upregulated and were significantly associated with both DFS and OS (Table 1). Both CD40 and CD40 L were significantly correlated with DFS and OS. Similar results were seen with CD74 and CIITA.

Genes	Disease free survival	Overall Survival
CD40	8.418e-06	1.345e-03
CD40LG	5.404e-04	3.441e-03
HLA-A	2.165e-02	8.704e-03
HLA-B	6.447e-03	1.331e-03
HLA-C	4.58e-02	7.793e-03
HLA-DRA	9.278e-06	2.124e-04
HLA-DRB1	5.967e-02	6.479e-03
HLA-DRB3	3.448e-02	6.479e-03
HLA-E	6.247e-03	1.608e-03
HLA-F	2.279e-04	2.234e-03
HLA-G	5.122e-04	2.73e-02
CD74	1.09e-03	9.178e-03
CIITA	6.775e-03	3.778e-02

Conclusions: Aberrant expression of the MHC I and II pathway in TNBC tumor cells may initiate and support an antitumor immune response that improves OS and DFS. Activation of the CD40/CD40L pathway supports better prognosis via pro-apoptotic signaling as well as augmenting B-cell involvement in antitumor response. Association of CIITA with both OS and DFS indicates its significant role as regulator of both MHC pathways in TNBC.

1841 Analysis of DNA Methylation in Breast Cancer for Field Effect Using Contralateral Tissue as the Reference

Rahul M Jawale, Chelsey A Mullen, Kelly J Gregory, Eva P Browne, Giovanna M Crisi, Christopher N Otis, Sallie S Schneider, Brian T Pentecost, Kathleen F Arcaro. Baystate Medical Center, Springfield, MA; University of Massachusetts, Amherst, MA; New York State Department of Health, Albany, NY.

Background: The field cancerization effect is generally understood as the presence of molecular alterations within histologically non-malignant tissue in the vicinity of a tumor that predisposes the normal tissue to cancer. Aberrant DNA methylation, an early event in cancer etiology, has been shown to be a robust molecular marker of cancerization in 'normal' tissue. For the present study we had access to tumor, and 'normal' tissue samples from both the affected, ipsilateral, and the contralateral breasts of women undergoing bilateral mastectomies. This provided a robust platform for initial analysis of the field of cancerization, with contralateral breast tissue serving as a reference point. However, our long-term aim is to define biomarkers that can be analyzed in the tumor tissue and be used to estimate whether a significant field of cancerization is present.

Design: Laser capture microdissection was used to obtain tumor epithelial cells, ipsilateral normal epithelial cells (distant from the tumor) and contralateral normal epithelial cells from FFPE tissue sections. High quality DNA was extracted from the cells of the three tissue types of eight women. DNA methylation values for over 850,000 CpGs were obtained with the Infinium Methylation EPIC array (Illumina). Beta values were analyzed in Genome Studio using both a candidate gene approach and global comparisons.

Results: Comparison of DNA methylation of 50 candidate genes including ARRDC3, AREG, CCND2, FGFR1, ID4, LTF, NDRG2, SFRP1, and WIF1 identified a group of 4 women whose normal tissue demonstrated a strong field cancerization effect and a group whose tissue did not have a cancerization field. Analyses comparing global DNA methylation in tumor tissues from the two groups are ongoing to identify biomarkers within breast tumors that predict the presence of a field of cancerization.

Conclusions: The recent trend among women diagnosed with unilateral breast cancer to choose contralateral prophylactic mastectomy, provides an opportunity to use contralateral tissue as a reference in defining the field cancerization effect and will aid in the discovery of tumor biomarkers that predict field cancerization. Our goal is to establish testing that can optimize strategies for applying post surgical adjunct therapies.

1842 SMAD4 Mutation Hotspot Analysis and Concomitant Key Cancer-Related Gene Mutation Profile in a Large Cohort of Colorectal Adenocarcinoma Using Next Generation Sequencing Approach

Ryan D Jones, David Dittmann, Nike T Beaubier, Juehua Gao, Guang-Yu Yang. Northwestern University, Chicago, IL.

Background: SMAD4 is mutated in 10-35% of colorectal cancers (CRC), and is often thought to be a late event in tumorigenesis. However, some studies demonstrate SMAD4 mutations in early stage disease which may confer a worse prognosis. Germline mutations in SMAD4 codon 361 have been implicated in a subset of juvenile polyposis syndrome, which portends an increased risk for gastrointestinal malignancy. This study utilizes next generation sequencing (NGS) of a unique profile of tumor-related genes together with immunohistochemistry (IHC) for DNA mismatch repair proteins and morphologic findings to further interrogate the role of SMAD4 in a large single institution cohort of CRC.

Design: Utilizing the Northwestern Memorial Hospital (NMH) clinical CRC cohort, a total of 242 CRC have been analyzed using NGS approach since 2015. Of these, 25 harbor a mutation in SMAD4 of either known pathogenicity or unknown status. Evaluation of protein expression for MLH1, PMS2, MSH2, and MSH6 was performed using IHC with proper controls.

Results: Our NMH cohort showed a frequency of SMAD4 mutations of 10.3%(25/242). Hotspot analysis for SMAD4 shows 40%(10/25) harbor a genetic alteration at the common codon 361, 88%(22/25) have missense mutations, 8%(2/25) have frameshift mutations, and one has a nonsense mutation. One case shows two point mutations at codons 352 and 523. Among the SMAD4-mutant CRC concomitant mutations include KRAS 52%(13/25), BRAF 16%(4/25), NRAS 4%(1/25), p53 44%(11/25), and PIK3CA 12%(3/25). SMAD4-mutant CRC lost expression of one or more DNA mismatch repair proteins in 16%(4/25), including two cases with BRAF mutations. These tumors localized with 36%(9/25) in the right colon, 60%(15/25) in the left colon, and one unique case from the urachus. Morphologic analysis demonstrates 48%(12/25) were moderately to poorly differentiated (high-grade) with 68%(17/25) either stage III or IV at the time of diagnosis, and 36%(9/25) demonstrate mucinous features.

Conclusions: Using NGS approach, our results demonstrate that concomitant mutation in p53 and RAS pathway genes (including KRAS, BRAF and NRAS) is a common genetic even in SMAD4-mutant CRC, indicating mutant SMAD4 in collaboration with mutant p53 and RAS is crucial leading to aggressive colon carcinogenesis. Since the high frequency of codon 361 mutations implies a potential relationship with juvenile polyposis syndrome, further study is warranted. As many of these tumors behave aggressively, SMAD4 status at the time of diagnosis may be of value as a prognostic indicator.

1843 22-Gene Signature for Distinguishing Lung Squamous Cell Carcinoma from Head and Neck Squamous Cell Carcinoma

Farah Khalil, Yin Xiong, Anthony Magliocco, Soner Altiok. H. Lee Moffitt Cancer Center and Research Institute, Tampa, FL.

Background: Primary squamous cell carcinoma (SCC) arising in the lung is morphologically indistinguishable from primary SCC arising in the head and neck area. SCC arising in the head and neck location can metastasize to the lungs and it becomes increasingly difficult to diagnose primary SCC from metastatic SCC in such situations. We have developed and validated a 22-gene signature that distinguishes SCC arising in the lung from SCC arising in the Head and Neck area.

Design: A total of 268 lung SCC samples and 38 head and neck SCC samples from Moffitt Cancer Center Total Cancer Care (TCC) database were used as the training dataset. The gene expression data are on HuRSTA chips, each with 60607 probe sets for 25587 genes. Unpaired t-tests were performed to identify significantly differentially expressed genes for lung vs. head-and-neck SCC. The top 22 most differentially expressed genes were selected for PCA (Principal Component Analysis) analysis. The first principal component (PC1) of the 22 genes was used as the signature which was first self-validated on the training dataset with 33 out of 38 correctly identified as "head-and-neck" (sensitivity = 86.8%) and 254 out of 268 correctly identified as "lung" (specificity = 94.8%).

The signature was further validated on external datasets publicly available at GEO and TCGA databases, with 130 SCC lung cancer samples from GSE4573, 134 SCC lung cancer samples from TCGA and 96 SCC head-and-neck cancer samples from GSE31056, total of 666 samples.

Results: The signature correctly identified all of the 130 samples of GSE4573 as "lung" (specificity = 100%), all the 134 samples of TCGA data as "lung" (specificity = 100%), and 88 out of the 96 SCC head-and-neck samples as "head-and-neck" (sensitivity = 91.7%).

Conclusions: This 22-Gene expression profile can assist in distinguishing primary lung SCC from metastatic head and neck SCC. This will make a significant impact on patient managment and outcome.

1844 Effect of Inactivation of HK1, HK2, and HK3 Genes in Colorectal Cancer and Melanoma Cell Lines

Anna Kudryavtseva, Maria Fedorova, Irina Karpova, Nadezhda Volchenko, Maria Chernichenko, Dmitry Sidorov, Anastasiya Snezhkina, Dmitry Kalinin. Engelhardt Institute of Molecular Biology, Russian Academy of Sciences, Moscow, Russian Federation; National Medical Research Radiological Centre, Ministry of Healthcare of the Russian Federation, Moscow, Russian Federation; A.V. Vishnevsky Surgery Institute of the Russian Ministry of Healthcare, Moscow, Russian Federation.

Background: The switch from oxidative phosphorylation to glycolysis in proliferating cancer cell even under aerobic conditions has been shown first in 1926 by Otto Warburg. Today "Warburg effect" is known as a metabolic phenotype, a hallmark of malignant tumors. This shift is associated with alterations in signaling pathways involved in energy metabolism, including glucose uptake and fermentation, and regulation of mitochondrial functions. It has been shown that many genes encoding glycolytic enzymes are dysregulated in cancer. Hexokinases (HKs), which catalyze the first step of glycolysis, have been identified to play a role in tumorigenesis of human colorectal cancer (CRC) and melanoma. However, the mechanisms of HKs in the promotion of tumor growth remain elusive. The purpose of this study is to investigate the effect of silencing hexokinase genes (HK1, HK2, and HK3) in colon cancer and melanoma.

Design: Cell line HT29, RKO, HCT116, CW480, and HCT15 were used for colon cancer as well as Ksen, Kor, Z, and Cher were used for melanoma. shRNA lentiviral plasmid vectors PLSLP-HK1, PLSLP-HK2, and PLSLP-HK3 were constructed and then transfected separately or co-transfected into cells.

Results: The results indicated that shRNA-mediated attenuation of HK2 and HK3 separately, as well as one together led to increased apoptosis rates of cancer cells and decreased glucose metabolism. HK1 gene inactivation did not result to significant changes in apoptotic rate or cells growth. Co-transfection by shRNA vectors against HK1, HK2, and HK3 together resulted in a rapid cell death by apoptosis.

Conclusions: Thus, our results suggest that HK2 and HK3 genes are the key therapeutic targets for reducing aerobic glycolysis. This study shows a promising strategy for colorectal and melanoma cancer therapy. This work was financially supported by grant 14-15-01083 from the Russian Science.

1845 Molecular Mechanisms Underlying Formation of Carotid Body Tumor Aggressive Phenotype

Anna Kudryavtseva, Dmitry Kalinin, Anastasiya Snezhkina, Alexander Golovyuk, Mikhail Zhestkov, Ekaterina Zhevelyuk, Oleg Stepanov, Alexey Dmitriev, Anatoly Pokrovsky, Boris Alekseev, Andrew Zaretsky, George Krasnov. Engelhardt Institute of Molecular Biology, Russian Academy of Sciences, Moscow, Russian Federation; National Medical Research Center of Radiology, Ministry of Healthcare of the Russian Federation, Moscow, Russian Federation; A.V. Vishnevsky Institute of Surgery, Moscow, Russian Federation; Shemyakin-Ovchinnikov Institute of Bioorganic Chemistry, Russian Academy of Science, Moscow, Russian Federation.

Background: Carotid body tumors are paragangliomas located near carotid bifurcation. Most of them are benign, though 10-15% of the tumors are recurrent and can form metastases. The study of the molecular mechanisms leading to malignant transformation is one of the most important tasks.

Design: We performed transcriptome and exome sequencing of 28 carotid body tumors using Illimina HiSeq 2000. Read preprocessing, alignment, counting, SNP calling and annotation was performed with PPLine toolkit. Differential expression analysis was done using edgeR Bioconductor package. Gene Ontology biological process, KEGG pathways enrichment and visualization were performed using topGO, clusterProfiler and pathview packages.

Results: We demonstrated that higher values of Ki67 is associated with hyperactivation of MAPK cascade, block of pathways responsible for cell differentiation (including activin receptors), increased inflammatory and immune response, overexpression of NF-kB, TNF-α, Jun, PI3K, mTOR. Higher CD117 values is primarily associated with dysregulation of cell adhesion and migration, which is directly linked to metastasis. Higher expression of p27 is followed with activation of pro-angiogenic and pro-inflammatory pathways. Driver mutations in SDHx genes and RET proto-oncogene are also accompanied with increased activity of angiogenic, immune-related and inflammatory pathways, and (only SDHx) alterations in extracellular matrix organization mechanisms, cell adhesion, which is also related to metastatic potential. Driver mutations in KMT2D are most probably associated with the formation of Warburg phenotype: the tumors with mutated KMT2D were characterized with suppressed oxidative phosphorylation against the background of down-regulated PGC-1α (activator of mitochondrial biogenesis) and overexpressed genes responsible for glucose transport and its regulation (GLUT1, PID1, IRS1, PIK3R1).

Conclusions: We revealed a set of molecular mechanisms underlying linkage between ki67, p27 and CD117 status, driver mutations and tumor progression as well as formation of aggressive phenotype. This work was supported by ICGEB grant no.CRP/15/010.

1846 mir-182*, mir-183, and mir-143 Are Deregulated in Endometrial Endometroid Cancers

Yong Li, Raja Luthra, Jianhua Hu, Li Shen, Russell R Broaddus, Erika Resetova, Yun Wu, Constance T Albarracin. University of Texas Health Science Center, Houston, TX; The University of Texas MD Anderson Cancer Center, Houston, TX.

Background: Molecular alterations in PTEN and microsatellite instabilty genes have been well described in endometrial endometrioid carcinomas (EEC). However, EEC lacking mutations in the above-mentioned genes suggest that other pathways exist in endometrial cancers. MicroRNAs (miRNAs) are a small class of nonecoding RNAs that can suppress mRNA translation leading to decrease in target protein levels. In recent years, studies have shown altered miRNAs expression in cancers. Some miRNAs are upregulated in tumors versus normal tissues and act as oncogenes. In this study, we will investigate the role of miRNAs in the pathogenesis of EEC and will identify putative targets of miRNA regulation.

Design: Five pairs of normal endometrial cancer and adjacent normal endometrial samples were applied to Human MicroRNA Panel v1.0 (Early Access, PE Applied Biosystems, Foster City, CA) TaqMan Low-Density Arrays. The analysis of miRNA predicted targets were determined by using the algorithms TargetScan and PicTar.

Results: MiRNA gene expression of a panel of 365 human miRNAs was evaluated in 5 pairs of endometrioid cancers and adjacent benign endometrium. Analysis of the data from the 5 pairs of samples revealed several miRNAs that were significantly altered. Differentially expressed miRNAs with p values from <0.0003 to 0.006 with 20-fold to more than 80-fold for the downregulated miRs and 10-fold to 95-fold for the upregulated miRNAs. We further evaluated three miRs which demonstrated the most statistically significant deregulation. Three of the deregulated miRNAs (miR-182*, miR-183 and miR-143) were further validated by mature miRNA-specific real-time qPCR . Quantitative real-time qPCR analysis was performed on 5 normal endometrium and 35 EEC patients. Real-time qPCR analysis revealed that miR-182* was up-regulated in 93% of EECs, miR-183 was up-regulated in 90% of EECs when compared with normal tissue, and miR-143 was down-regulated in 76% of EECs.

Because miR-183 was one of the most frequently up-regulated miRNAs in the EEC tumors we next to examine its putative human protein-coding gene targets. Using computational analysis, we have identified candidate targets based on 3'UTR regions and have begun to characterize them.

Conclusions: Our studies demonstrate significant alterations in miRNA expression in EEC and support a role for miNRAs in the pathogenesis of EEC. As we begin to identify the targets of these miRNAs, this can be useful in understanding alternative pathways of endometrial carcinogenesis.

1847 Identification of Sarcoma Fusion Genes by Multiplex Detection of Aberrant 3' to 5' Expression Ratios

Adrian Marino-Enriquez, Frank C Kuo, Michele Baltay, George Demetri, Neal I Lindeman, Jonathan Fletcher, Lynette M Sholl. Brigham and Women's Hospital, Boston, MA; Dana Farber Cancer Institute, Boston, MA.

Background: Translocation-associated sarcomas are characterized by recurrent oncogenic gene fusions that serve as diagnostic markers. The detection of diagnostic gene fusions may be challenging due to the large number of genes involved and wide variability in the genomic breakpoints. Fusion events often lead to differential expression levels of exons 3' *vs.* 5' to the genomic breakpoints. We designed a NanoString RNA-based molecular barcoding assay to detect aberrant 3' to 5' expression ratios in sarcoma patient samples.

Design: A custom set of 60 probes was designed to target 3' and 5' exons of *EWSR1*, *NR4A3*, *YWHAE*, *NUTM2A, CIC* and *DUX4* transcripts. Seven probes spanning specific gene fusion junctions and 7 control gene probes were included. Proof-of-concept experiments were performed on 12 sarcoma samples (5 FFPE, 7 frozen) with known gene fusions, including 6 Ewing sarcomas, 3 extraskeletal myxoid chondrosarcomas (EMCS), 2 high-grade endometrial stromal sarcomas (HG-ESS), and 1 CIC-DUX4 round cell sarcoma. Two FFPE dedifferentiated liposarcomas (DDLPS) were used as controls. RNA was extracted (Qiagen) and 200 ng were hybridized to the custom probe set following the NanoString nCounter Fusion Gene Analysis protocol. Images were processed and analyzed with a NanoString nCounter instrument and nSolver software.

Results: Eleven of 12 sarcoma samples demonstrated diagnostic 3' to 5' expression imbalances or fusion transcripts. By contrast, these alterations were not detected in the DDLPS controls. Aberrant 3'/5' expression ratios were detected in 7 of 10 sarcomas with known fusion genes, involving *EWSR1* in 3 of 6 Ewing sarcoma, *EWSR1* or *NR4A3*

in each of 3 EMCS, and *NUTM2A* in each of 2 HG-ESS. One CIC-DUX4 round cell sarcoma had markedly increased levels of *DUX4* expression. *YWHAE* and *CIC* showed variable expression, with no demonstrable 3'/5' expression imbalances. Five Ewing sarcomas, including 2 lacking 3'/5' *EWSR1* imbalance, had *EWSR1* fusion transcripts, as demonstrated by increased counts of junction-specific probes (counts range 44-1740).
Conclusions: Initial studies suggest that sarcoma fusion genes can be detected in frozen and FFPE tissues using a multiplex NanoString 3'/5' expression imbalance assay. However, assay sensitivity is increased by inclusion of fusion-specific probes.

1848 Assessment of *HER2 A*mplification Using NGS - Comparison with FISH and IHC

Rebecca M Marrero Rolón, Kyung Park, Pan Zhang, Mark A Rubin, Helen Fernandes. Weill Cornell Medicine, New York, NY.
Background: *HER2* gene amplifications have been identified in a variety of cancer types including breast, gastric, prostatic, and bladder cancers. The presence of *HER2* amplification has major prognostic and therapeutic implications. The Oncomine Comprehensive Panel (OCP) is a targeted NGS platform that can detect Copy Number Alterations in 49 genes. It can also identify clinically relevant single nucleotide variants in 73 DNA hotspots and 23 gene fusions in RNA simultaneously from FFPE tumor tissue. The OCP is directly aligned with the NCI- MATCH clinical trial. This study aims to validate the performance of OCP for accurate identification of *HER2* amplification in solid tumors.
Design: The cohort consisted of 20 surgical specimens including 5 breast ductal carcinomas, 8 urothelial carcinomas, 3 gastroesophageal adenocarcinomas, 2 prostatic cancers, 1 colonic adenocarcinoma, and 1 serous adenocarcinoma of the uterus. Eighteen of 20 cases had confirmed *HER-2* amplification by whole exome sequencing (WES). All of 20 cases were subjected to NGS using the OCP and the data was analyzed by the Ion Reporter™ Software 5.0. Results of *HER2* amplification by FISH and protein overexpression by IHC were available for 10 and 11 cases with known *HER2* amplification, respectively. The amplification status of *HER2* using the different testing methodologies was compared.
Results: Concordance in *HER2* status was seen in 85% (17/20) of the cases when OCP and WES were compared. There were three discordant cases in which OCP did not detect *HER2* amplification. These three represented "borderline" cases which did not meet one of the two criteria to be interpreted as amplified (copy number greater than 4 and greater than 5% confidence score at the lower bound). The first discordant case showed moderate protein expression by IHC and amplification by FISH. The second case had amplification by FISH; no IHC was available. No IHC or FISH data was available for the third case. In the samples with available FISH data, there was 100% concordance with WES results. By IHC, negative/weak protein expression was seen in 3 cases and moderate/strong expression was seen in 8 cases.
Conclusions: This study demonstrated that the *HER2* status was correctly identifed by OCP for the majority (85%) of the cases. The thresholds of the bioinformatics pipeline for calling amplifications need to be set by comparison with results obtained from established methodologies. For the borderline cases, it is prudent to reflex the results for confirmation with an orthogonal method.

1849 Novel Multiparametric High Resolution Flow Cytometry to Sort Cell-Specific and Size-Specific Extracellular Vesicles

Terry Morgan, Jared Cobb, David Edwards. OHSU, Portland, OR.
Background: There is intense interest in developing new methods to perform liquid biopsies of tumors using blood samples. This is possible because tumors release millions of lipid encapsulated extracellular vesicles (EVs)/ml into the blood stream. The term EVs includes small exosomes (50-150 nm) and larger sub-micron sized microparticles. Concentrations of these EVs appear to be related to tumor size and stage. Moreover, EVs contain protein, RNAs and fragments of DNA that are suitable for -omics research and diagnostics. Progress in the field has limited, however, by the lack of cell and size-specific rapid isolation methods. To address this issue, our group has developed a new multiparametric high resolution flow cytometry (HRFC) sorting method that can reliably identify, quantitate, and purify cell- and size-specific EVs from any tumor of interest.
Design: Submicron-sized polystyrene beads (100, 160, 200, 240, 300, 500, 900nm) were used as sizing and sorting efficiency controls. We used placental EVs present at high concentrations in maternal blood to validate the method and then began experiments testing pancreatic ductal adenocarcinoma specimens compared with negative controls. Sorted EVs of various sizes and from various cell types (e.g. placenta, platelets, pancreas) were characterized by electron microscopy, and used to test whether there was enrichment of target-specific protein and microRNA markers.
Results: Cell and size-specific EVs can be resolved and sorted to a high level of purity (>99%) using as little as 10 ul of plasma to generate 10^5 isolated EVs (10^7/ml) within 10 minutes. Sorted placental EVs are positive for exosome markers like CD9 and Annexins. They are positive for trophoblastic markers like FLT-1 and placental-related microRNAs. Electron microscopy confirms sorted EVs are the expected size, purity, and concentration. CD41 positive platelet EVs are present in similar concentrations, but are a distinctly different size, ranging from 350-500nm. In pilot studies, we have also used EpCAM and CD55 to highlight pancreatic cancer EVs present in tissue positive controls, which are 150-350nm in size. Pancreatic cancer blood analyses comparing proven ductal adenocarcinoma cases with negative controls are pending.
Conclusions: Using blood samples from pregnant women as a model for enriched "tumor" EV populations we have validated our new multiparametric HRFC sorting method. This novel technology provides a rapid means to characterize, count, and isolate cell and size-specific EVs from patient plasma.

1850 Co-Mutations of Driver Oncogenes in Untreated Primary Lung Adenocarcinomas (ADCs) and Clinical Correlations

Doreen Nguyen, Minghui Ao, Frederic Askin, Ed Gabrielson, Gang Zheng, Qing K Li. The Johns Hopkins Medical Institutions, Baltimore, MD.
Background: Recent progress in cancer genetics has changed the landscape of lung cancer, including development of targeted therapies for patients whose tumors harbor specific genetic alterations. In the same tumor, co-mutations have been found in <1% of cases, and occur more often during the course of targeted therapy (e.g. *EGFR* T790M mutation). Co-mutations in untreated lung ADCs, however, have not been well studied. In this study we examined the oncogenic driver gene co-mutations and clinicopathologic features of untreated primary lung ADCs.
Design: A retrospective search of the JHMI Surgical Pathology Data Systems was conducted for primary lung ADCs resected over a 3-year period. Only cases which had molecular testing performed using a targeted NGS lung panel (*AKT, BRAF, EGFR, ERBB2, KRAS, NRAS*, and *PIK3CA* genes) were included. Briefly, DNA was extracted, subjected to multiplex PCR amplification using Ion AmpliSeq Cancer Hotspot Panel (v2). and sequenced with the Ion PGM 200 Sequencing Kit and Personal Genome Machine (PGM).
Results: 206 primary lung ADCs with molecular studies were identified. Among them, 8 untreated (3.9%) tumors were found to have 2 or more driver mutations detected by NGS. See Table 1

Case	Age/ Sex	EGFR muta-tions	KRAS mutations	PIK3CA mutations	BRAF mutations	NRAS mutations	Othermuta-tions
1	44/F	p.L730R					ERBB2 (p.V777_ G778insGSP)
2	37/M	p.R98Q (rs17289589)	G12D				
3	70/M	p.G719A	G12C				
4	56/F			D350N ex4	E611Q		
5	76/F		G12C			G48A	
6	67/F	A767_ S768insSVD		E545K ex9			
7	73/F	P.V774fs, p.H773dup		N345I ex4			
8	73/F		G12C	E545K ex9			

5 of the 8 cases had *EGFR* mutations with concurrent *KRAS* (2 cases), *PIK3CA* (2 cases), or ERBB2 (1 case) mutations, while 3 had co-mutations in *PIK3CA/BRAF*, *PIK3CA/KRAS* and *KRAS/NRAS*. The majority of tumors (87.5%) were moderately to poorly differentiated, and some had solid/papillary morphology. Among 8 patients, 6 were female. 6 of 8 patients also had smoking history.
Conclusions: The prevalence of co-mutations in untreated primary lung ADCs may be higher than previous observations. We identified a subgroup of untreated primary ADCs whose tumors harboring 2 or more distinct oncogenic driver mutations. Further studies are needed to determine the significance of these findings and their potential impact.

1851 Genome-Wide Analysis of Copy Number Alteration in Well-Differentiated Papillary Mesothelioma

Kyung Park, Jin Chen, Robert Taub, Alain C Borczuk. Weill Cornell Medicine, New York, NY; Columbia University Med Ctr, New York, NY.
Background: Well-differentiated papillary mesothelioma (WDPM) of the peritoneum is a rare disease with benign clinical course. The three most frequent genetic alterations in malignant mesothelioma are homozygous 9p21 (*CDKN2A*) deletions, heterozygous loss of the *NF2* gene (22q12.3), and *BAP1* (3p21.1) loss and mutations. We investigated copy number alterations (CNAs) in WDPM and peritoneal epithelioid mesothelioma (PEM) to help distinguish these histologic entities.
Design: Seven cases of WDPM (1 snap frozen and 6 FFPE) and 48 cases of PEM (41 snap frozen and 7 FFPE) were manually micro-dissected for tumor-rich areas with an 18-gauge needle from 8 µm thick sections. DNA from the frozen and FFPE tissues were analyzed by Affymetrix Genome Wide Human SNP array 6.0 (500 ng DNA) or OncoScan CNV FFPE Assay (80 ng) for copy number. Data analysis was performed using Nexus Copy Number Software v.7.5 (BioDiscovery, Hawthorne, CA).
Results: Broad overview of the CNA plot demonstrated that PEM had more frequent aneuploidies spanning larger regions than WDPM.

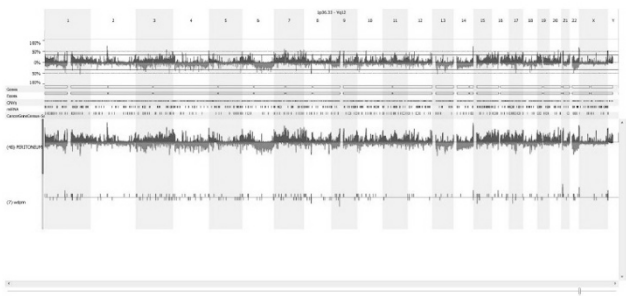

Loss of *CDKN2A*, *NF2,* and *BAP1* was observed in 27%, 21%, and 37.5% of PEM. In contrast, no WDPM showed copy number loss in these three genes. Direct comparison of WDPM and PEM revealed regions of copy number differences at p-value of <0.05 and difference threshold of 30%.

	Chr	Gene	PEM (%)	WDPM (%)
Copy number gain	3	PIK3CA	50	14
	4	KIT	42	14
	7	EGFR	71	14
	7	PMS2	31	0
	7	CARD11	40	0
	7	TNS3	43	0
	11	HRAS	48	14
	11	CCND1	40	0
	17	CANT1	50	0
	19	FSTL3	50	0
	19	STK11	44	14
Copy number loss	3	BAP1	37.5	0
	3	SETD2	44	0
	13	FLT3	62.5	14

High copy number gains and homozygous losses were not seen in WDPM. Overall, PEM shows more frequent regions of gain than loss, but WDPM does not show frequent genomic imbalances.

Conclusions: Copy number loss of *CDKN2A*, *NF2,* and *BAP1* is seen less frequently in PEM than in pleural mesothelioma, and are not seen in WDPM. Detection of large regions of aneuploidy favors a malignant mesothelioma over WDPM and could be helpful in diagnostically challenging cases.

1852 Expanding Therapeutic Options for Patients with Lung Adenocarcinomas Using Oncomine Comprehensive Panel

Kyung Park, Hung Tran, Xiaojun Feng, Mark A Rubin, Helen Fernandes. Weill Cornell Medicine, New York, NY; Englander Institute for Precision Medicine, New York, NY.

Background: Detection of driver mutations has become the standard of care for therapeutic management of patients with various tumors. The Oncomine Comprehensive Panel (OCP) detects single nucleotide variants (SNVs), insertion/deletion (indel), and copy number alterations (CNAs) in DNA and gene fusions in RNA from tumor enriched FFPE tissue. NCI-MATCH is a clinical trial that uses OCP to identify actionable mutations and assigns treatment based on the genomic alterations. In this study, we attempted to compare the therapeutic utility of the143-gene OCP to the 50-gene Ion Ampliseq Cancer Hotspot Panel (CHP) for identification of variants in non-small cell lung cancers (NSCLC).

Design: In 2016, 290 of the 369 (79%) NSCLCs that were sequenced by CHP at NYPH Molecular Laboratory harbored reportable hotspot variants and 79 cases (21%) were found to have no variants. DNA from 35 cases with no CHP variants were randomly selected and sequenced by OCP. Six of 35 cases harbored ALK fusion detected by FISH. Twenty-two cases were surgical specimens (core biopsies/resections) and 13 cases were cytology specimens (fine need aspirate/pleural fluid). Twenty-five cases were primary and 10 cases were metastatic tumors. The tumor cellularity ranged from 10-80% and DNA concentration from 1.34-116 ng/ul. The data obtained was analyzed by the Ion Reporter™ Software 5.0.

Results: There was 100% concordance between the two panels in that OCP also did not detect hotspot variants covered by CHP. Eight of 35 cases had newly identified SNVs/indels. Four specimens had variants in the NF1 gene and one case harbored a documented ERBB2 p.S310F variant that was reported to be responsive to trastuzumab *in vitro*. CNAs including recurrent amplifications in chr 8, 11 and 12, and deletions in chr 11, 13, and 17 were detected in 13 cases. In total, 15/35 cases had additional genomic alterations detected by OCP, 7 of which could serve as potential qualifiers for NCI-MATCH treatment arms. The targets included SNVs in ERBB2 and NF1 genes, FGFR1/2/3 aberrations, and CCND 1/2/3 amplifications. Additional clinical trials for tumors with CDK4 and AKT1 alterations were identified. In two patients, concurrent ALK fusions were present.

Conclusions: Collectively, OCP was able to potentially extend therapeutic alternatives to 7/35 (20%) patients with NSCLC. The targeted NGS panel can increase the enrollment in clinical trials, broaden current knowledge on cancer therapy, and change clinical management.

1853 Personalized Preclinical Cancer Models to Guide Precision Medicine

Chantal Pauli, Benjamin D Hopkins, Davide Prandi, Reid Shaw, Andrea Sboner, Verena Sailer, Rachele Rosati, David J Pisapia, Rema A Rao, Juan Miguel Mosquera, Brian Robinson, Olivier Elemento, Himisha Beltran, Francesca Dimichelis, Christopher Kemp, Carla Grandori, Lewis Cantley, Mark A Rubin. Englander Institute for Precision Medicine, Weill Cornell Medicine, New York, NY; Meyer Cancer Center, Weill Cornell Medicine, New York, NY; Cure First and SEngine Precision Medicine, Seattle, WA.

Background: Precision oncology is a clinical approach aimed towards tailoring treatment strategies for patients based on the genetic profile of each patient's cancer. Our Institute developed a robust Precision Cancer Care Program, which integrates whole exome sequencing (WES) with a living biobank, enabling high throughput drug screening on patient derived tumor organoids (PDTO) and in vivo testing in patient derived xenografts (PDX). Through the development of a living biobank with patient derived samples we hope to facilitate the integration of genetic data with drug screening in order to help guide clinical decision-making and to fuel next generation research.

Design: PDTOs are established from fresh tumor specimens and characterized according to our cytology, histology and genomic platforms. Characterized PDTOs are expanded, biobanked, used for *in vitro* drug screening and implanted in nude mice for the *in vivo* testing of potential drug candidates.

Results: To date WES of 769 tumor-normal pairs, 56 tumor derived organoid cultures from 18 different solid tumor types and 19 PDX models have been established. Mean success rate in generating PDTOs is 35%, depending on specimen quality and tumor type (e.g. endometrial cancer 70%, metastatic prostate cancer 5%) and 85% for PDX development from tumor organoids. Tumor morphology and molecular profiles show good concordance among PDTOs, PDTXs and native tumor tissues. We so far performed high throughput drug screening (up to 160 compounds exposed to 6-8 different drug concentrations) on 8 PDTO lines. 7 of these lines were subjected to combination drug screens with candidate compounds from the initial screens and/or compounds indicated by the genetic data at their approximate IC30 dose. We nominated several targeted small molecules and novel combinations that have been tested in corresponding xenograft.

Conclusions: This precision medicine approach nominates novel therapeutic opportunities for cancer patients who have exhausted standard of care options. The integration of genomic data with drug screening from personalized preclinical cancer models does not only guide precision cancer care, it also fuels next generation research and has been implemented for Clinical Trial development in our Institution.

1854 Luminal Androgen Receptor and Androgen Receptor-High Triple-Negative Breast Cancers Are Genetically Similar to Luminal B Breast Cancers

Ashwini Raghavendra, Kathleen A Burke, Jisun Kim, Felipe Geyer, Samuel H Berman, Charlotte K Ng, Simon Powell, Britta Weigelt, Sarat Chandarlapaty, Jorge Reis-Filho. Memorial Sloan Kettering Cancer Center, New York, NY; University Hospital Basel, Basel, Switzerland.

Background: Triple-negative (TN) breast cancers (TNBCs) can be classified into seven gene expression subtypes. The luminal androgen receptor (LAR) is one of these subtypes, and is characterized by expression of androgen receptor (AR) and transcriptomic features of AR-pathway activation. Our aim was to investigate the genomic landscape of TNBC of LAR subtype and to compare it with other subtypes of TN and non-TN breast cancers.

Design: Gene expression and targeted sequencing data from the METABRIC study (n=1992) were obtained. TNBCs were identified (n=320) and classified into the seven TNBC molecular subtypes and according to AR mRNA expression levels. Mutation profiles of LAR and AR-high TNBCs were compared to those of non-LAR/ non-AR-high TNBCs, respectively, and of non-TNBCs classified as luminal A, luminal B and HER2-enriched by PAM50.

Results: Of 320 TNBCs, 8% were classified as LAR. We classified as AR-high those TNBCs with AR expression levels above the top 20 percentile. High levels of AR were associated with but not restricted to TNBCs of LAR subtype. LAR TNBCs as compared to non-LAR TNBCs displayed a significantly higher frequency of somatic mutations affecting *PIK3CA* (46% vs 12%)*, AKT1* (25% vs 0%), *GATA3* (8% vs 0%) and *CDH1* (8% vs 1%), which are genes commonly mutated in luminal cancers. In contrast, LAR TNBCs as compared with luminal, luminal A and luminal B displayed a significantly higher rate of mutations in *TP53* (66% vs 17%, 12% and 25%) and *AKT1* (25% vs 4%, 5.5% and 4%). Similar results were obtained when comparisons were performed between AR-high TNBCs and AR-low TNBCs and luminal cancers. *AKT1* was the sole gene significantly more frequently mutated in LAR than in AR-high non-LAR TNBCs. Notably, mutations affecting *PIK3CA* and *AKT1* were mutually exclusive in LAR or AR-high TNBCs, and 81% of LAR TNBCs displayed mutations in PI3K pathway genes (*PIK3CA*, *AKT1*, *PTEN* or *PIK3R1*). Interestingly, the pattern of *TP53* mutations differed between LAR TNBCs and TNBCs of other subtypes.

Conclusions: High levels of AR expression are not restricted to TNBCs of LAR subtype. The transcriptomic similarities between LAR and luminal breast cancers are mirrored by similarities at the genetic level, in particular by a high rate of mutations affecting *PIK3CA* and *AKT1*. LAR TNBCs are genetically similar to AR-high non-LAR TNBCs.

1855 *ALK* Fusions in Cancers Other Than Non-Small Cell Lung Cancer Occur in a Wide Variety of Tumor Types and Respond Vigorously to Anti-ALK Targeted Therapy

Jeffrey Ross, Siraj M Ali, Julia A Elvin, Alexa Schrock, James Suh, Jo-Anne Vergilio, Shakti H Ramkissoon, David Fabrizio, Garrett Frampton, Vincent Miller, Philip Stephens, Laurie M Gay. AlbanyMed Col, Albany, NY; FoundationMed, Cambridge, MA.

Background: Genomic fusions of the anaplastic lymphoma kinase gene (*ALK*) are a well-established therapy target for patients with NSCLC. In a survey of 92,784 clinical cases we determined the prevalence of *ALK* fusions in non-NSCLC tumors and their responsiveness to anti-ALK targeted therapies.

Design: Comprehensive genomic profiling (CGP) of 92,784 relapsed and metastatic malignancies was performed using a hybrid-capture, adaptor ligation based next generation sequencing assay to a mean coverage depth of >600X. Tumor mutational burden (TMB) was calculated from a minimum of 1.2 Mb of sequenced DNA.

Results: 1,036/92,784 (1.1%) cases featured *ALK* GA of which 704 (68%) were fusions (Table). 574 (82%) of *ALK* fusions were found in NSCLC and 128 (18%) in non-NSCLC: 40 in sarcomas including 19 non-uterine and uterine leiomyosarcomas; 19 in CUP; 15 in colon and small intestinal carcinoma; 18 in NHL; 6 in pancreatic carcinomas; 5 in thyroid papillary carcinomas; 4 in GYN epithelial tumors; 3 in gliomas and histiocytosis; 2 each in breast, head and neck, small cell lung carcinomas, mesotheliomas and myelomas; and 1 each in adrenal neuroblastoma, gallbladder, renal clear cell and prostatic carcinomas and melanoma. Mean age in *ALK* fusion pos non-NSCLC was 60.6 years with 78 (60%) female and 50 (40%) male patients. *EML4* was the fusion partner in 86 (67%) non-NSCLC cases. Non-fusion *ALK* alterations

including subs, indels and amplifications were more frequent in non-NSCLC than NSCLC (p<0.001). *ALK* fusion pos non-NSCLC had significantly lower TMB (mean 5.01 mutations/Mb) than non-*ALK* altered non-NSCLC (p=0.006). There were only 4 (3%) cases with high TMB (TMB > 20 mutations/Mb) including all 3 (2%) of cases with high MSI. In >10 *ALK* fusion pos non-NSCLC major responses to approved anti-ALK kinase inhibitor therapies were seen.

	ALKAlterations	ALKFusions	ALKShort Variants	ALKAmplifications
TotalCases	1,036	704	286	85
NSCLC	653	574	75	13
Non-NSCLC	383	128	183	61

*Each case can have more than 1 *ALK* alteration

Conclusions: Although uncommon, *ALK* fusions do occur in a wide variety of clinically advanced non-NSCLC malignancies and are most often identified in cases of sarcomas especially with smooth muscle differentiation, NHL, CUP, CRC, pancreatic and papillary thyroid cancers. These non-NSCLC *ALK* fusions typically have a low TMB, are less often associated with *EML4* and have universally been associated with responsiveness to anti-ALK targeted therapies.

1856 Stratification of Tumors with POLE Mutations by Mutations in Additional DNA Polymerases

Joanne K Rutgers, Fangjin Huang, Beatrice Knudson. Cedars Sinai Medical Center, Los Angeles, CA.

Background: Tumors with mutations in POLE, a DNA polymerase responsible for leading strand synthesis, are associated with an ultramutator phenotype. POLE mutations, in particular in the exonuclease domain, are best understood in colorectal (CORE) and uterine cancers (UCEC) and are associated with a prominent immune infiltrate and favorable prognosis. There are 15 DNA polymerases and co-mutations in cancers has not been well studied

Design: We analyzed exome sequence data from 15 cancer types with POLE mutations(PANCAN) in The Cancer Genome Atlas (TCGA). We grouped cases by mutation status of the most commonly mutated polymerases. Mutation burden, microsatellite instability (MSI) status, tumor stage, disease free survival and immune scores were calculated.

Results: Amongst the 15 DNA polymerases, the highest rates of mutation and co-mutation with POLE were POLQ and REV3L(POLZ). 36% of POLE mutant tumors, predominantly CORE, stomach (STAD) and UCEC carried mutations in POLQ (E/Q), POLZ/REV3L (E/Z), or all three (E/Q/Z). Compared to the POLE-only mutant tumors, tumors with E/Q, E/Z, and E/Q/Z mutations possessed significantly higher overall mutation frequencies ($p < 0.001$) (figure 1) and increased frequencies of mutations within the POLE exonuclease domain ($p = 0.013$). E/Q, E/Z, and E/Q/Z mutant CORE, STAD and UCEC demonstrated 100% disease-free survival (figure 2) even if mutations occurred outside the POLE exonuclease domain ($p = 0.003$).

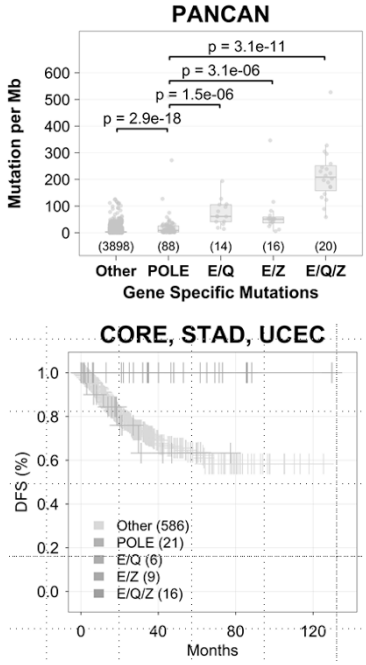

These tumors did not display a higher immune score than tumors with MSI, suggesting that other mechanisms improve disease-free survival.

Conclusions: Our results demonstrate that other polymerases may contribute to the ultramutator phenotype. Further studies should focus on the roles on POLQ and Rev3L(POLZ) as predictive or therapeutic targets.

1857 High Prevalence of Germline DNA-Repair Defects (DRD) in Advanced Cancer Patients Detected Through Precision Medicine Program

Verena Sailer, Tuo Zhang, Juan Miguel Mosquera, David J Pisapia, Chantal Pauli, Brian Robinson, Rema A Rao, Joanna Cyrta, Rob Kim, Terra J McNary, Marc H Schiffman, David M Nanus, Scott T Tagawa, Andrea Sboner, Olivier Elemento, Himisha Beltran, Mark A Rubin. Weill Cornell Medicine, New York, NY.

Background: Precision medicine (PM) can uncover the molecular mechanisms that drive tumorigenesis hence identifying targetable somatic alterations in patients with advanced cancer. Recent publications suggest that germline DNA-repair defects may be prevalent in a higher frequency in patients with aggressive cancer. Here we report germline and somatic alterations in a large pan-cancer PM cohort.

Design: Patients with advanced and metastatic cancer were prospectively enrolled in an ongoing precision medicine clinical trial in New York between February 2013 and July 2016. Paired tumor/normal samples underwent whole exome sequencing (WES). RNAseq was performed on a subset of cases.

Results: 769 samples from 501 patients and a variety of metastatic (51.2%), recurrent (8.5%) and primary (40.3%) tumor sites were sequenced. Informative results were obtained for the majority of patients (93.6%). Metastatic samples revealed significantly more clinically relevant alterations (n=51) than primary/recurrent samples (39/34; p=0.001). The most prevalent copy number alterations were *CDKN2A* and *CDKN2B* deletions. Pathogenic germline DRD were detected in 6.7% of all patients. *BRCA1/2* were the most commonly mutated genes with a more than fourfold increase in frequency in our cohort as compared to the population frequency of 0.62% in the ExAC database which provides germline data from more than 60,000 individuals (Maxwell, KN et al., Population Frequency of Germline *BRCA1/2* Mutations, JCO, 2016).

Conclusions: In an unselected patient cohort with advanced and metastatic cancer, germline DRD are significantly more frequent than in the general population. The majority of cases also harbor clinically relevant somatic alterations. Our results justify enrolling advanced cancer patients for combined tumor/normal sequencing to identify actionable alterations. Importantly, the germline findings also contribute to the growing body of evidence that inherited alterations in DNA-repair mechanisms may be predictive of a more aggressive course of disease and has therapeutic implications including platinum or PARP inhibitors.

1858 The Prognostic Value of Serum Mi-301a Expression in Prostate Cancer

Devin K Sanders, Mohammed A Alghamdi, Youssef Khafateh, Chendil Damodaran, Houda Alatassi. University of Louisville School of Medicine, Louisville, KY.

Background: Serum prostate specific antigen (PSA) is commonly used for diagnosis and screening. PSA is of limited clinical utility due to poor sensitivity and specificity. Large number of false positives with traditional PSA testing lead many patients to undergoing unnecessary prostate biopsy. MicroRNAs (miRNAs) have previously shown their expression patterns are correlated with many types of cancer including prostate cancer. These small, noncoding RNA molecules are present in all human cells.

Design: The goal of this proposal is to identify a reliable, non-invasive biomarker that can distinguish patients with benign, indolent and aggressive prostate cancer in various clinical settings. A total of 21 serum samples from prostate cancer patients (5 AA, 15 Caucasian; mean age: 63) of prostate cancer with their clinical diagnosis were selected for this study. Total RNA was extracted from serum samples by using miRVana kit (Invitrogen) according to the manufacturer's instructions. cDNA was synthesized with miscript II kit (Quiagen). Real-time PCR was performed with Applied Biosystem using miScript RT II SYBR kit. The mature form of miRNAs was detected using the miRNA qPCR quantitation assay according to the manufacturer's instructions. The 18S/U6 was used as internal controls.

Results: We found significant (p=0.0058) differential expression of miR-301a in serum samples between benign prostate hyperplasia (BPH) and prostate tumors (Gleason, 6, 7, and 8-10). African American prostate patients were found to have higher expression of miR-301a than Caucasian patients, and patients with a positive family history of prostate cancer were found to have increased miR-301a expression compared to patients with no family history of prostate cancer. However, no difference in expression of miR301a was found in smokers vs. non-smokers. MiR-301a expression was correlated with clinical aggressiveness (Gleason stages) of the disease. Our ongoing experiments on paired prostate tumor tissues further validate our miR-301a expression in prostate cancer patients.

Conclusions: Our results suggest that miR-301a expression may prove a valuable tool for the diagnosis of prostate cancer in patients presenting with elevated PSA. Given the poor specificity of PSA, miR-301a could avoid unnecessary biopsy for men with PSA elevation due to non-malignant causes.

1859 HPV-Induced Changes to the EBV Life Cycle in an EBV/HPV Co-Infection Model Utilizing Organotypic Raft Culture

Mingxia Shi, Joseph T Guidry, Rona Scott. Louisiana State University Health Science Center, Shreveport, LA.

Background: Human papillomavirus-associated oropharyngeal squamous cell carcinoma (HPV+OSCC) exhibit distinct properties compared to other HPV-associated cancers arising in the anogenital tract, including high invasive potential and rapid progression. These unique characteristics implicate other factors besides HPV in malignant progression of HPV+OSCC. One candidate is Epstein-Barr virus (EBV), a ubiquitous oncogenic gammaherpesvirus present in oral lymphoid tissues in which the majority of OSCC occur. We questioned whether EBV/HPV co-infection could lead to alterations in viral life cycles that would favor malignant progression. EBV is dependent upon differentiation of the epithelium for completion of its life cycle, and HPV oncoproteins E6 and E7 are known to interfere with epithelial differentiation. We therefore hypothesized that HPV interrupts EBV replication via E6 and/or E7.

Design: To study EBV/HPV co-infection, we have used a physiologically relevant co-infection model utilizing organotypic raft culture in which epithelial cells are induced to differentiate in three-dimensional culture to recapitulates stratified epithelium in vivo. Tonsillar keratinocytes immortalized with HPV were infected with EBV via co-culture with EBV-positive Akata Burkitt's lymphoma cells. Rafts were harvested post-EBV infection and subjected to analysis of viral life cycles.
Results: Using this model, changes to HPV replication were not detected following EBV infection. In HPV-negative keratinocytes, robust EBV replication was observed. In contrast, a dramatic reduction in EBV DNA levels was observed in HPV-positive keratinocytes. Human telomerase-immortalized normal oral keratinocytes supported robust EBV replication in organotypic raft culture, suggesting a specific effect of HPV rather than immortalization on EBV. Additionally, we observed that expression of E7 was sufficient to decrease EBV DNA levels.
Conclusions: Our data implies that HPV, via expression of E7, decreases EBV DNA levels potentially via down-regulation of EBV replication. A decrease in EBV replication may signify a shift in the EBV life cycle toward viral latency, a stage characterized by persistent EBV infection. The ability of EBV to establish persistent latent infection in HPV-infected epithelial cells would contribute additional viral oncogene expression to explain the rapid development and progression of HPV+OSCC.

1860 A Digital Pathology Method to Identify All Forms of CTC

Cathy Spillane, Brendan Ffrench, Anthony Cooney, Carmel Ruttle, Anna Bogdanska, Noreen Gleeson, Feras Abu Saadeh, Waseem Kamran, Ciaran O'Riain, Ricahrd Flavin, Michael Gallagher, Cara M Martin, Orla Sheils, Sharon O'Toole, John J O'Leary. Trinity College Dublin, Dublin, Ireland; Coombe Women & Infants University Hospital, Dublin, Ireland; Dublin City University, Dublin, Ireland; St. James's Hospital, Dublin, Ireland.
Background: Disseminated malignancy is responsible for the majority of cancer-related deaths and circulating tumour cells (CTCs) play a central role in metastasis. CTCs are seen as an exciting new way to detect and monitor cancer, as they can be isolated from a simple blood sample, which is minimally invasive and can be acquired easily and repeatedly. As with any early technology, there are technical and diagnostic issues; including the dependency of CTC identification on epithelial markers, which are often lost during metastasis. This study aimed to overcome current marker based limitations and to evaluate CTCs in cancer patients.
Design: CTCs were isolated from whole blood of cancer patients (ovarian and breast) using ScreenCell®Cyto filtration devices. Filters were slide mounted, giemsa stained and digitised. Filters were then washed, immunofluorescently stained for epithelial (EpCAM/panCK), lymphocyte (CD45) and cancer characterising (Her3 or CD42b) markers, as well as DAPI (nuclear stain), and digitally imaged. Giemsa and 4-colour immunofluorescent digital images were processed *in silico*, generating a single z-stacked digital image for pathological review.
Results: This study developed a novel staining pipeline (CTC-5) combining histochemical and immunofluorescent staining, with whole slide imaging for robust identification, enumeration and characterisation of CTCs. CTC-5 was validated using peripheral blood from healthy donors with spiked-in cancer cell as controls. Subsequently, CTCs were isolated from patient samples, demonstrating that CTCs are highly heterogeneous, both between and within patient samples. CTCs with different morphologies, including single CTCs, doublets and microemboli, and molecular characteristics, including epithelial and/or Her3 marker positivity and negativity, were identified.
Conclusions: The CTC-5 approach overcomes current weaknesses in CTC characterisation. By combining histochemical staining with the current gold standard (EpCAM/panCK and CD45 staining) and an additional level of biomarker assessment (e.g. HER3 or CD42b), enables robust pathological assessment of CTCs.

1861 Patterns of Clonal Evolution in Colorectal Adenocarcinomas Characterized by Whole Exome Sequencing

Efsevia Vakiani, Ronak H Shah, Marc Attiyeh, Jinru Shia, Alvin P Makohon-Moore, Christine Iacobuzio-Donahue, David Solit. Memorial Sloan Kettering Cancer Center, New York, NY.
Background: A limited number of colorectal carcinomas (CRC) have undergone genomic profiling by massively parallel exome or genome sequencing with conflicting results. The goal of this study was to define the extent of genetic heterogeneity between primary tumors (PT) and matched liver metastases (LM) in patients presenting with synchronous and metachronous distant disease.
Design: The study included 10 patients who presented with metastases and whose tumors were resected prior to therapy and 10 patients who developed metastases ≥ 12 months (mean 18.7 months) following resection of their PT. All 40 tumors were microsatellite stable and among those patients that were treated (n=8) only one received an anti-EGFR inhibitor. DNA was extracted from frozen tumors as well as normal tissues and subjected to massively parallel whole exome sequencing (150x tumor coverage). Somatic single nucleotide variants (SNVs) and insertions and deletions (indels) were detected by MuTect and HaplotypeCaller. Variants were filtered for coverage (≥20 reads) and variant allele frequency (≥5%) and those detected in cancer related genes (CRG, based on pan-cancer analyses) were manually reviewed.
Results: There were no significant differences between patients presenting with synchronous and metachronous metastases in terms of age, gender, PT site and outcome. LM in all cases were clonally related to PT. The percent of alterations shared between PT and LM ranged from 22% to 82% (mean 55%) of all variants detected in a given patient. The results were similar when considering only CRG. In contrast, genomic concordance in genes mutated in ≥5% of TCGA CRC cases was 90%. Review of the 36 metastasis specific events detected in CRG did not identify any recurrently mutated genes and only 9 (25%) were found to be truncating or hotspots mutations. There were no significant differences in the level of genomic concordance between synchronous and metachronous cases.
Conclusions: Patterns of clonal evolution vary between CRC patients with resectable liver metastases with some LM showing early divergence from PT, while others show late divergence and limited genetic heterogeneity. These patterns can occur both in patients that present with metastases and those that develop LM subsequently. Despite the presence of substantial genetic heterogeneity in some cases potentially functional SNVs or indels in CRG are not frequent among metastasis specific events suggesting that the majority of driver alterations are early events that can be identified by genomic profiling of the PT.

1862 RAC2 Links B-cell Receptor Signaling and Cell Adhesion in Mantle Cell Lymphoma

Weige Wang, Madina Sukhanova, Dong Sheng, Mei Ming, Ailin Guo, Pin Lu, Jia Li, Xiaoqiu Li, Xiaoyan Zhou, Lynn Y Wang. the University of Chicago, Chicago, IL; Fudan University Shanghai Cancer Center, Shanghai, China; Fudan University Shanghai Medical School, Shanghai, China; Shanghai Institute of Materia Medica, Shanghai, China.
Background: Mantle cell lymphoma (MCL) is an incurable non-Hodgkin B-cell lymphoma. Ibrutinib has generated remarkable patients' response in large clinical trials and has been approved by FDA for the treatment of relapsed/refractory MCL patients. Ibrutinib works by targeting BTK kinase to inhibit B-cell receptor signaling. In addition, it inhibits interaction of tumor cells with their microenvironment by its effects on cell adhesion. However, the underlying mechanism is largely unknown.
Design: In this study, we used RNA-sequencing to identify pathways that have differential response to ibrutinib in cell lines that are either sensitive or resistant to Ibrutinib treatment. We then validate RNA-Seq finding using sensitive and resistant cell lines, animal models and human primary cells.
Results: We found that sensitivities of MCL cell lines to ibrutinib correlated well with cell adhesion phenotype. RNA-sequencing revealed that BCR signaling and cell adhesion programs were down-regulated by ibr in ibr-sensitive cells but not ibr-resistant cells. Among genes that are down-regulated in the BCR signature, we identified *RAC2* that is a known regulator of cell adhesion. We then examined RAC2 expression in primary MCL tumors by IHC and found that RAC2 was weakly expressed in 7/10 classic MCL tumors and strongly expressed in 3/3 aggressive MCL. In MCL cell lines, Ibrutinib down-regulated the expression of RAC2 and its association with BLNK, a component of early BCR signaling pathway, only in sensitive cells but not in resistant cells. siRNA knock-down of *RAC2* impaired the cell adhesion while exogenous introduction of *RAC2* attenuated ibr induced cell adhesion inhibition. In xenograft mouse model, mice treated with ibr showed slower tumor growth and reduced RAC2 expression. In primary human MCL cells, RAC2 was down-regulated by Ibrutinib that correlated well with cell adhesion impairment following Ibrutinib treatment.
Conclusions: Our findings suggest the RAC2 mediates the link between BCR signaling and cell adhesion and Ibrutinib inhibits cell adhesion via down-regulation of RAC2. Our study highlights the importance of cell adhesion in MCL pathogenesis.

1863 Cleaved NH_2-Terminal Villin Fragment Regulates Intestinal Cell Extrusion in the Villus Tip

Yaohong Wang, Sudeep P George, Seema Khurana. University of Tennessee Health Science Center, Memphis, TN; University of Houston, Houston, TX; Baylor College of Medicine, Houston, TX.
Background: The small intestinal epithelium is a dynamic tissue characterized by high cellular turnover rates. Cell extrusion in the villus tips plays a fundamental role in this process to maintain the intestinal epithelial architecture and homeostasis. Pathological changes in the enterocyte shedding has been linked to several bowel diseases including inflammatory bowel disease, bacterial infections, and colon cancer. Redistribution of actin and actin associated proteins is the crucial step in cells destined to undergo extrusion. Villin is a major actin-modifying protein that is associated with the microvillar actin filaments and is expressed in significant amounts in gastrointestinal epithelial cells.
Design: MDCK cells expressing full length wild-type villin were used in vitro study. The actin severing activity of full length villin (VIL/WT) as well as the NH2-terminal villin fragment (VIL/NT) was determined by analyzing the rate of decrease in fluorescence of pyrene labelled actin. Villin knockout (VKO) mice and their wild type (WT) littermates were subjected to 8 Gy radiation and apoptotic cells were analyzed 4h post-treatment. Apoptosis was measured by counting TUNEL-positive nuclei, as well as histologically in H&E-stained sections.
Results: Villin is cleaved in the GI epithelium as cells migrate along the crypt-villus axis, a lack of expression of the COOH-terminal fragment of villin at the villus tip and expression of only the NH2-terminal fragment of villin along the length of the villus including the villus tips showed the possibility of degradation of the COOH terminal fragment of villin. In vitro, cleaved NH2 terminal villin fragments depolymerize actin in an unregulated manner (calcium independent), which would disrupt the cell junctions/attachment and induce cell extrusion from the villus tips. After radiation, cell extrusion was seen from the villus tips of WT mice but no cell extrusion could be documented from the villus tips of the VKO mice.
Conclusions: Expression of full-length and cleaved villin correlates with the cell's position along the crypt-villus axis and determines the ability of the cells to undergo apoptosis and extrusion. Our study describes for the first time a molecular mechanism to regulate extrusion from the villus tips. This process appears to be uniquely adapted to the epithelial cells, using an epithelial cell specific actin regulatory protein namely, villin.

1864 Computer Extracted Features of Nuclear Shape and Architecture Predict Oncotype DX Risk Categories for Early Stage ER+ Breast Cancer

Jon Whitney, Andrew Janowczyk, German Corredor, Hannah Gilmore, Anant Madabhushi. Case Western, Cleveland, OH.

Background: Oncotype DX (ODX) is a 21 gene assay used to stratify women with early stage ER+ breast cancer into low, intermediate and high risk categories, high risk being women who would benefit from adjuvant chemotherapy. In this work we explored the use of computer extracted features of nuclear architecture and morphology from routine H&E images to predict ODX risk categories for lymph node negative ER+ BCa.

Design: The dataset contains 178 BCa patients with H&E stained whole slide images of low, intermediate, and high ODX risk. Nuclei were segmented and classified as either epithelial or stromal using Deep Learning models, and had nuclear architectural features (median, standard deviation of the edge lengths of nuclear graphs), as well as nuclear shape features extracted.

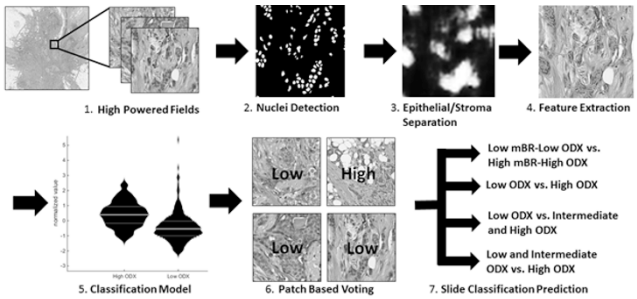

Figure 1. QH ODX Classification Process

These features were used to train a random forest classifier and evaluated via three fold cross-validation. The four experiments we performed were discriminating 1) Low ODX (LODX) and Low modified Bloom-Richardson (mBR) grade vs. High ODX (HODX) and High mBR grade (LL vs. HH), 2) LODX vs. HODX, 3) LODX vs. Intermediate (Int.) and HODX, and 4) LODX & Int. ODX vs. HODX.

Results: Classification performance was judged for each risk category using Area Under the Curve (AUC) values. The most clearly distinct groups (LL vs. HH) were most consistently classified correctly, with an AUC of 0.77.

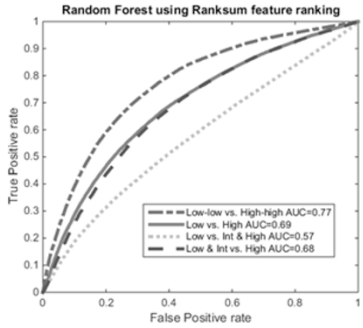

Figure 2. ROC curves for each set of ODX risk categories separated

The highest performing features for separating LODX from HODX were epithelial nuclei architectural features captured by the Cell-Cluster Graph (CCG), shape of stromal nuclei were also found to be important. The standard deviation of CCG Edge Length yielded an AUC=0.67 for separating LODX from HODX.

Conclusions: We showed that computer extracted features of epithelial nuclear architecture and stromal shape from H&E images can distinguish ODX risk category.

1865 Tissue Based Proteomics on Paraffin Embedded Tissue: A Feasible Means of Identifying and Following Biomarkers in Breast Cancer

Richard Wong, Leslie Timpe, Richard Schwab, Farnaz Hasteh, Bruce Macher, Ten-Yang Yen. University of California San Diego, San Diego, CA; UC San Diego, San Diego, CA; San Francisco State University, San Francisco, CA.

Background: The identification and integration of biomarkers into cancer patient care is a cornerstone in the promise of personalized medicine. The evaluation of genetic profiles via sequencing and protein phenotypes via immunohistochemistry are well established protocols in pathology labs. Proteomics by mass spectrometry offers a powerful tool for identifying and following multiple biomarkers, but is not yet integrated into the standard evaluation of patient samples. In this study we establish a protocol with proof of principle for incorporating mass spectrometry into the normal workflow of breast cancer specimens processed into formalin fixed paraffin embedded (FFPE) tissue.

Design: 55 specimens of human FFPE breast tissue were obtained from the Cooperative Human Tissue Network and institutional tissue biorepository. Tissue included breast carcinomas with patient matched normal breast tissue as well as unmatched breast carcinoma samples. For each specimen two 10 micron FFPE sections were cut and treated with xylene and rehydrated. Sections were then incubated in citrate buffer. Trypsin digestion was carried out, proteolytic peptides were recovered, concentrated, and analyzed by LC/MS/MS. Proteins were identified using Mascot, Proteome Discoverer, Scaffold, and Sequest programs.

Results: From all the proteins identified, 290 were selected after being detected in greater than 1/3 of the total samples. Hierarchical clustering analysis showed that profiling these 290 proteins distinguished normal from malignant tissue. Significance analysis further identified 28 proteins that are differentially expressed in the normal vs malignant sapmles. One of these proteins, P11021 (Grp78) has been identified in the literature as a candidate predictive biomarker for response to anthracyclines and platinum based drugs.

Conclusions: Identification and trending of biomarkers is an important part in the management of cancer patients. Genetic and immunophenotypic characterization of tumors have been integrated seamlessly in the current standards of care. The results of this study highlight tissue based proteomics as a practical and feasible means for identifying and following protein biomarkers during the treatment course of a patient's cancer.

1866 A Study of Metastatic Low-Grade Clear Cell Renal Cell Carcinoma by Targeted Next-Generation Sequencing

Sina Zomorrodian, Minghao Zhong, David Y Zhang, Jian Zhuge, Taliya Farooq. New York Medical College at Westchester Medical Center, Valhalla, NY; Icahn School of Medicine at Mount Sinai, New York, NY.

Background: Fuhrman grade is an important criteria in the grading of Clear Cell Renal Cell Carcinoma (CCRCC), however metastasis is still seen in tumors with low clinical grade. As of yet there is no criteria to stratify high risk metastatic CCRCC with indolent types. In this study, we utilize targeted next generation sequencing to study the molecular profile of high risk low grade CCRCC.

Design: Metastatic CCRCC cases were reviewed from 2010 to 2016 on the Softpath database and selected on the basis of low histologic grade (Fuhrman nuclear grade 1 & 2) and positivity for metastasis. FFPE tissue was used for targeted next-generation sequencing by the Illumina Truseq Amplicon Panel which targets 48 commonly mutated genes. The genetic variance profile was reviewed for the cases (n=4) and genes containing mutations with a frequency of $\geq$ 5% and < 95% were selected. Selected mutated genes were subsequently reviewed for frequency of occurrence within the cases, and compared with genes listed in a "Comprehensive molecular characterization of clear cell renal cell carcinoma" analyzed by the Cancer Genome Atlas Research Network (CGARN).

Results: Of the mutated genes, 7 were identified in all 4 cases (APC, ATM, FBXW7, GNAQ, KDR, PIK3CA, RET, SMAD4 & TP53) with freq=x, 5% $\leq$x <95%. Of these genes, 2 (PIK3CA & TP53) were previously identified by CGARN.

Conclusions: The genes identified in this study all contained mutations with known deleterious effects. Hence, these genes (both novel and previously reported) are potentially involved in the pathogenesis of metastasis in low-grade CCRCC.

Pediatric Pathology

1867 Genome-Wide DNA Methylation Profiling in the Diagnosis of Pediatric Ewing Sarcoma, Osteosarcoma, and Synovial Sarcoma

Fang Bu, Benjamin Cooper, Peter Wu, Marc Ladanyi, Richard G Gorlick, Matthias Karajannis, Kristen M Thomas, Matija Snuderl. New York University Medical Center, New York, NY; Memorial Sloan Kettering Cancer Center, New York, NY; The Children's Hospital at Montefiore, New York, NY.

Background: Pediatric sarcomas, constituting 15-20% of pediatric cancers, are a unique diagnostic challenge. Only a subset, including Ewing and synovial sarcomas, harbor pathognomonic genomic alterations. Epigenetic modifications such as changes in DNA methylation are gaining recognition as a primary oncogenic mechanism. Genome-wide methylation profiling could identify biologically and clinically relevant subgroups of tumors, including those without oncogenetic fusions.

Design: We developed a random forest based classifier using the top 400 differently methylated genes for a pilot cohort (N = 36) of three common pediatric bone and soft tissue sarcomas. Using the Illumina Infinium Human Methylation450 BeadChip Array (450K array) platform, we performed genome-wide DNA methylation analysis on 10 Ewing sarcomas, 15 osteosarcomas, and 11 synovial sarcomas, including formalin-fixed paraffin-embedded, frozen, and fresh tissue. Unsupervised hierarchical clustering analysis was performed to compare methylation signatures among tumor types.

Results: On molecular studies, 6 of 11 synovial sarcomas had an SYT fusion and all 10 Ewing sarcomas had an EWSR/FLI1 fusion. Unsupervised hierarchical clustering analysis showed distinct DNA methylation profiles for each sarcoma type. Synovial sarcomas clustered together, EWSR fusion sarcomas made a second cluster, and osteosarcomas formed a third. We validated our classifier against publicly available methylation data from the TCGA-SARC and TARGET-OS databases for synovial and osteosarcomas, respectively, and obtained 98.9% concordance.